bioRxiv preprint doi: https://doi.org/10.1101/2024.02.29.582698; this version posted February 29, 2024. The copyright holder for this preprint (which was not certified by peer review) is the author/funder, who has granted bioRxiv a license to display the preprint in perpetuity. It is made available under aCC-BY-NC-ND 4.0 International license.

Characterisation of prophages in *Clostridium clostridioforme*: an understudied component of the intestinal microbiome

Suzanne Humphrey[1,2]*, Angeliki Marouli[2,3], Katja Thümmler[2], Margaret Mullin[4] and Daniel M. Wall[2]

[1]Strathclyde Institute of Pharmacy and Biomedical Sciences, University of Strathclyde, Glasgow, G4 0RW, United Kingdom

[2]School of Infection and Immunity, College of Medical and Veterinary Sciences, University of Glasgow, Glasgow, G12 8TA, United Kingdom

[3]Current address: School of Dental Sciences, Framlington Place, Newcastle University, Newcastle upon Tyne, NE2 4BW, United Kingdom

[4]University of Glasgow, CAF Electron Microscopy Unit (MVLS College Research Facilities), Glasgow G12 8QQ, United Kingdom

*Corresponding author email address: Suzie.Humphrey@strath.ac.uk

Key words

Bacteriophage, *Clostridium clostridioforme*, *Enterocloster clostridioformis*, microbiome, dysbiosis, Transmission Electron Microscopy (TEM)

bioRxiv preprint doi: https://doi.org/10.1101/2024.02.29.582698; this version posted February 29, 2024. The copyright holder for this preprint (which was not certified by peer review) is the author/funder, who has granted bioRxiv a license to display the preprint in perpetuity. It is made available under aCC-BY-NC-ND 4.0 International license.

Abstract

Genome sequencing of *Clostridium clostridioforme* strain LM41 revealed the presence of an atypically high proportion of mobile genetic elements for this species, with a particularly high abundance of prophages. Bioinformatic analysis of prophage sequences sought to characterise these elements and identify prophage-linked genes contributing to enhanced fitness of the host bacteria in the dysbiotic gut. This work has identified 15 prophages, of which 4 are predicted to be intact, 2 are predicted to be defective, and 9 are unclassified. qPCR analysis revealed spontaneous release of four of the LM41 prophages into the culture supernatant, the majority of which had morphology akin to podoviruses when visualised using Transmission Electron Microscopy. We observed diversity in the lysogeny mechanisms utilised by the prophages, with examples of the classical λ-like CI/Cro system, the ICE*Bs*1 ImmR/ImmA-like system, and the Mu-like C/Ner system. Classical morons, such as toxins or immune evasion factors, were not observed. We did, however, identify a variety of genes with roles in mediating restriction modification and genetic diversity, as well as some candidate genes with potential roles in host adaptation. Despite being the most abundant entities in the intestine, there is a dearth of information about phages associated with members of the microbiome. This work begins to shed light on the contribution of these elements to the lifestyle of *C. clostridioforme* LM41.

bioRxiv preprint doi: https://doi.org/10.1101/2024.02.29.582698; this version posted February 29, 2024. The copyright holder for this preprint (which was not certified by peer review) is the author/funder, who has granted bioRxiv a license to display the preprint in perpetuity. It is made available under aCC-BY-NC-ND 4.0 International license.

Introduction

The intestinal microbiome, consisting of bacteria, viruses, fungi and protozoa, plays an intimate role in contributing to the health and nutrition of its host. The microbial partners in this commensal relationship aid the host in a variety of ways, including nutrient extraction[1], modulation of the immune and nervous systems via the activity of microbially-derived factors[2–4], and by providing a barrier against colonisation of the gut with intestinal pathogens[5,6]. Disruption of the diversity and richness of the microbiome (known as dysbiosis) can occur through a variety of factors, including host genetics, antibiotic use, and diet and lifestyle[7–9]. Several diseases that include a dysbiosis component are associated with signature reductions and blooms of particular bacterial species[10–13]. Currently, the reasons why some species can adapt to and proliferate more readily in response to microbiome perturbation remain unclear. *Clostridium clostridioforme* (recently reclassified as *Enterocloster clostridioformis*) has been noted to proliferate rapidly in the intestines of people with a variety of conditions associated with gut dysbiosis, including obesity, type 2 diabetes and autism spectrum disorder[13–15]. Additionally, Western or high fat diets, which are established risk factors in obesity and type 2 diabetes development, significantly increase *C. clostridioforme* occurrence in the gut[16], while the species has also been seen to increase post-antibiotic treatment[16,17].

We recently described a novel strain of the gut commensal *C. clostridioforme*, LM41[18]. In addition to carrying multiple novel secondary metabolite biosynthetic gene clusters (BCGs), LM41 hosts several novel mobile genetic elements (MGEs), including a 192 kb plasmid, 7 integrative conjugative elements (ICEs), 5 integrative mobilisable elements (IMEs), 27 IS66 transposases, and 29 putative prophages; it is highly probable that at least some of these elements contribute to niche adaptation within the dysbiotic gut environment.

Bacteriophages (phages) are an integral facet of bacterial lifestyles and are widely distributed throughout the human gut microbiota. Estimates of the abundance of phage in the intestine are thought to approximately equal that of bacteria[19] suggesting important roles for these viruses in regulating bacterial population dynamics, contributing to horizontal gene transfer (HGT) within and between bacterial species, and altering their bacterial hosts' fitness

bioRxiv preprint doi: https://doi.org/10.1101/2024.02.29.582698; this version posted February 29, 2024. The copyright holder for this preprint (which was not certified by peer review) is the author/funder, who has granted bioRxiv a license to display the preprint in perpetuity. It is made available under aCC-BY-NC-ND 4.0 International license.

in the intestinal environment. While virulent phages undergo a strictly lytic replication cycle which results in phage-mediated bacterial cell death, temperate phages can engage in a secondary lifestyle known as lysogeny. Lysogeny occurs when temperate phages integrate into the bacterial chromosome following infection of the cell, generating a prophage. The prophage remains dormant in the bacterial lysogen, replicating as part of the bacterial chromosome until an environmental signal triggers its induction into the replicative, lytic pathway. Lysogeny was historically considered to be a parasitic relationship on behalf of the phage, however, increasingly studies are demonstrating that temperate phages offer their host bacteria important advantages as trade-offs for the inherent risk associated with their carriage. Integration of a prophage into its bacterial host's chromosome can permit expression of prophage-encoded factors that alter the host cell phenotype in a process known as lysogenic conversion. These can include virulence factors, such as the Shiga toxin carried by *E. coli* STEC Stx phages, the cholera toxin carried by the *Vibrio cholerae* CTX phage, and a variety of staphylococcal toxins carried by *S. aureus* phages and phage-inducible chromosomal islands[20,21]. Other well-characterised prophage-encoded factors include the SopE SPI-1 type 3 secretion system effector proteins of *Salmonella* Typhimurium SopEφ, and immune system evasion proteins *eib* (serum resistance; λ-like phage) in *E. coli* and *oac* (O-antigen acetylase; Sf6 phage) in *Shigella flexneri*[20]. More recently, prophages have become recognised for the protective effects that their lysogenic lifecycles can have for their host bacterial cell, with some phages encoding factors to modify their host cell's surface in order to prevent further infection by exogenous phage, e.g. the *gp15*-encoded superinfection exclusion protein of *E. coli* phage HK97[22], or simply by occupying attachment sites within their lysogen to prevent integration of superinfecting phage. In the latter case, expression of the CI repressor molecule by the resident phage appears to be sufficient to block the replicative cycle of infecting phages[23], leading to destruction of the infecting phage when its ability to integrate is impeded by the resident prophage occupying the *att*C site in the bacterial chromosome. Furthermore, at the whole population level, carriage of prophages can be beneficial in enabling lysogenic

bioRxiv preprint doi: https://doi.org/10.1101/2024.02.29.582698; this version posted February 29, 2024. The copyright holder for this preprint (which was not certified by peer review) is the author/funder, who has granted bioRxiv a license to display the preprint in perpetuity. It is made available under aCC-BY-NC-ND 4.0 International license.

communities to sample genetic material from other cells owing to the stochastic nature of phage induction[24].

Here, we sought to gain an understanding of the biology of bacteriophages in *C. clostridioforme* LM41. We used a combination of bioinformatic and experimental approaches to reveal the genome structure, functionality, and morphology of these prophages. Our findings indicate that *C. clostridioforme* strain LM41 is poly-lysogenic for 15 prophages, the majority of which are predicted to be functional or potentially functional, and many of which carry genes with roles in facilitating restriction modification and genetic diversity, possibly contributing to the apparent proclivity of LM41 for DNA acquisition. We show that 4/15 phages are spontaneously released from LM41 under standard culture conditions, with diversity observed in their morphologies.

Materials and Methods

Prophage identification and annotation

For details of *C. clostridioforme* LM41 whole genome sequencing, refer to Kamat *et al* (2024). Putative prophage sequences present in the LM41 genome were identified using PHASTER[25]. Manual interrogation of PHASTER hits was performed using SnapGene Viewer software (version 5.3, www.snapgene.com) and BLASTp software (https://blast.ncbi.nlm.nih.gov), with hits deemed to be prophages or prophage remnants if they contained gene clusters conforming to one or more of the classical phage genome functional modules (lysis-lysogeny control, DNA replication, packaging and capsid, tail, and lysis). Prophage regions were annotated using Pharokka[26] (https://usegalaxy.eu/root?tool_id=pharokka) and PhageScope[27] (https://phagescope.deepomics.org). Pharokka parameters: Pharokka DB v.1.2.0 (downloaded at 2023-08-07 07:02:08:010437); Phanotate gene predictor; E-value threshold for mmseqs PHROGs database, 1E-05. Genome completeness assessments were performed with PhageScope. Phage regions were categorised based on completeness scores: a completeness score of 100 was categorised as ‘functional’; a completeness score of >60-<100 was categorised as ‘unknown’; and a completeness score of <60 was categorised as

bioRxiv preprint doi: https://doi.org/10.1101/2024.02.29.582698; this version posted February 29, 2024. The copyright holder for this preprint (which was not certified by peer review) is the author/funder, who has granted bioRxiv a license to display the preprint in perpetuity. It is made available under aCC-BY-NC-ND 4.0 International license.

'defective'. Manual inspection of annotated genomes led us to categorise a further 5 prophages as 'unknown' based on unusual features predicted to affect viability (see results). For detection of putative promoter sites within lysogeny modules, PhagePromoter[28] (Galaxy server galaxy.bio.di.uminho.pt) was used to search both strands with the following parameters: threshold, 0.5; host bacterial genus, 'other'; phage type, 'temperate'. Phage family (myovirus, siphovirus, podovirus) was selected for each phage as assigned in Table 2. Only hits with scores in the range 0.87-1.0 were considered. All hits are presented in Supplementary File 1.

Bacterial strains and culture conditions

C. clostridioforme LM41 was grown in Fastidious Anaerobe Broth (FAB; Neogen) or on FAB agar (FAB supplemented with 1.5% agar [Formedium]) under anaerobic conditions (10% H_2, 10% CO_2, 80% N_2, 60-70% humidity) in an A35 workstation (Don Whitely Scientific) at 37°C. All media was reduced prior to inoculation. Overnight cultures were first prepared by inoculating 5 ml of pre-reduced FAB with a single colony of LM41 from a freshly streaked plate. Fresh, pre-reduced FAB was subsequently inoculated 1:50 (v/v) with the overnight culture and allowed to grow for up to 24h under anaerobic conditions.

Induction of *C. clostridioforme* LM41 prophages using DNA-damaging antibiotics

C. clostridioforme LM41 was diluted 1:50 from an overnight culture into 50 ml FAB and grown to an optical density via absorbance at 600 nm (OD600) of 0.7 under anaerobic conditions at 37°C. Cultures were induced by addition of DNA-damaging antibiotics to a final concentration of 3 µg/ml: mitomycin C (Sigma), norfloxacin (Sigma) or ciprofloxacin (Sigma). An uninduced control culture was also included. All cultures were grown for a further 16-18 h post-induction. Cultures were then centrifuged at 2800 x *g* for 30 min and the supernatants were filtered through 0.22 µm filters to remove remaining bacterial cells.

Extraction and quantification of encapsidated DNA from induced samples

bioRxiv preprint doi: https://doi.org/10.1101/2024.02.29.582698; this version posted February 29, 2024. The copyright holder for this preprint (which was not certified by peer review) is the author/funder, who has granted bioRxiv a license to display the preprint in perpetuity. It is made available under aCC-BY-NC-ND 4.0 International license.

Filtered supernatants were treated with 10 µg/ml DNase I (Sigma) and 1 µg/ml RNase A (Sigma) for 30 min at room temperature, then NaCl was added to a final concentration of 1 M. After incubation for 1 h on ice, the mixture was centrifuged at 11,000 x *g* for 10 min at 4ºC and the supernatant was transferred to a fresh tube. Polyethylene glycol (PEG) 8000 was added to the supernatant at a final concentration of 10% (w/v) and the mixture was incubated overnight at 4ºC. Phages were precipitated from the mixture by centrifugation at 11,000 x *g* for 20 min at 4ºC, with the final pellet resuspended in 1 ml phage buffer (1 mM NaCl, 0.05 M Tris pH 7.8, 1 mM $MgSO_4$, 4 mM $CaCl_2$). For extraction of encapsidated DNA, each sample was subject to a further DNase I treatment (20 µg/ml) for 1 h at room temperature to degrade any non-encapsidated DNA in the sample. DNase activity was stopped by addition of 20 mM ethylenediaminetetraacetic acid (EDTA) (Sigma), with incubation for 10 min at 70ºC. Capsids were then opened by addition of 50 µg/ml proteinase K (Sigma) and 1% SDS to each sample, with incubation at 55ºC for 1 h, mixing at 20 min intervals. The samples were subsequently transferred to fresh microcentrifuge tubes and an equal volume of phenol-chloroform-isoamyl alcohol (25:24:1; Sigma) was added to each. Samples were mixed by vortexing followed by centrifugation at 18,000 x *g* for 5 min at 4ºC to allow separation of the phases. The upper phase was transferred to a fresh microcentrifuge tube and the DNA was precipitated by addition of 0.1 volumes of 3 M sodium acetate (pH 5.2) and 2.25 volumes of ice-cold 100% ethanol at -80ºC for 16-18 h. Samples were centrifuged at 18,000 x *g* for 20 min at 4ºC, and the pellets were washed once with ice-cold 70% ethanol before centrifuging once more. After discarding the supernatant, the pellets were air dried prior to resuspension in 50 µl nuclease-free water. Resuspended pellets were stored at 4ºC for 16-18 h to allow sufficient time for solubilisation of DNA in each sample, then the DNA was quantified using a DS-11 spectrophotometer (DeNovix Inc, Wilmington, USA).

Detection of spontaneous LM41 phage release by qPCR

The presence of phages in the bacterial supernatant was quantified using qPCR. All oligonucleotide sequences are shown in Table 1. *C. clostridioforme* LM41 was grown for 24 h

bioRxiv preprint doi: https://doi.org/10.1101/2024.02.29.582698; this version posted February 29, 2024. The copyright holder for this preprint (which was not certified by peer review) is the author/funder, who has granted bioRxiv a license to display the preprint in perpetuity. It is made available under aCC-BY-NC-ND 4.0 International license.

in FAB under anaerobic conditions at 37ºC. The culture was centrifuged at 2800 x *g* for 30 min and the supernatant filter sterilised through a 0.22 µm syringe filter to remove bacterial cells and debris. Equal volumes of supernatant were treated with 10 µg/ml DNase I (Sigma) in DNase activating buffer (50 mM Tris-HCl, pH7.5; 10 mM $MgCl_2$) to degrade non-encapsidated DNA, or with an equal volume of DNase activating buffer (without DNase I) as a control. In parallel, 200 ng of LM41 genomic DNA was digested to confirm enzymatic activity of the DNase enzyme mix (see Supplementary Figure 1). Samples were incubated at 37ºC for 1 h, then heated at 85ºC for 15 min to inactivate the DNase enzyme and lyse any phage capsids present to release encapsidated DNA. Samples were used immediately as template for qPCR analysis.

qPCR was performed using a CFX Connect Real-time qPCR system (Biorad). Twenty microlitre reaction mixtures were prepared using the Luna® Universal qPCR Master Mix kit (New England Biolabs) as follows: 10 µl 2X Luna® qPCR master mix, 7.0 µl nuclease-free H_2O, 1.0 µl forward primer (final concentration 3 µM), 1.0 µl reverse primer (final concentration 3 µM), and 1.0 µl of either DNase-treated or control supernatant as template. Three technical replicates were performed per sample per primer set. Cycling conditions were: 95ºC for 3 min, then 40 cycles of 95ºC (10 sec), 60ºC (10 sec), 65ºC (30 sec). For comparison of relative quantities of phage in the sample, the $2^{-\Delta\Delta Cq}$ method was used, with *C. clostridioforme* LM41 small ribosomal protein 10 (*s10p*) gene used as the housekeeper.

Purification of LM41 phages for Transmission Electron Microscopy

1.6 L of *C. clostridioforme* LM41 was grown for 24 h in FAB under anaerobic conditions at 37ºC. The culture was centrifuged at 2800 x *g* for 30 min and the supernatant was filtered through a 0.22 µm filter to remove remaining bacterial cells. The supernatant was treated with 10 µg/ml DNase I for 1 h at room temperature, then NaCl was added to a final concentration of 1 M. After incubation for 1 h on ice, the mixture was centrifuged at 11,000 x *g* for 10 min at 4ºC. Polyethylene glycol (PEG) 8000 was added to the supernatant at a final concentration of 10% (w/v) and the mixture was incubated overnight at 4ºC. Phages were precipitated from the

bioRxiv preprint doi: https://doi.org/10.1101/2024.02.29.582698; this version posted February 29, 2024. The copyright holder for this preprint (which was not certified by peer review) is the author/funder, who has granted bioRxiv a license to display the preprint in perpetuity. It is made available under aCC-BY-NC-ND 4.0 International license.

mixture by centrifugation at 11,000 x *g* for 20 min at 4°C, with the final pellet resuspended in 1 ml phage buffer (1 mM NaCl, 0.05 M Tris pH 7.8, 1 mM $MgSO_4$, 4 mM $CaCl_2$) and stored at 4°C.

Transmission Electron Microscopy (TEM)

Carbon filmed 400 mesh copper TEM grids (AGAR Scientific) were glow discharged using a Quorum Q150TES high vacuum coater (20 mA, 30 sec). Three microlitres of precipitated phage suspensions were applied to the resulting hydrophilic carbon support films and allowed to adsorb for 3 min. Excess volume was removed by blotting and the grids were fixed for 5 min in 1 % (w/v) paraformaldehyde in phosphate-buffered saline solution. Grids were washed three times with distilled water for 30 sec, then stained with 0.5 % (w/v) uranyl formate solution for 30 sec. Sample grids were air dried at room temperature and then were examined using the JEOL 1400 FLASH TEM microscope running at 80 kV at the University of Glasgow CAF Electron Microscopy Unit (MVLS College Research Facilities). Digital images were captured at 50-150 K magnification using JEOL TEM Centre software v.1.7.26.3016 and inbuilt 2K X 2K CCD Flash camera. Particle dimension measurements were performed using ImageJ software v. 1.54h (https://imagej.net/ij/).

Statistical analysis

Statistical analyses were performed as described in the figure legends. All analyses were performed using GraphPad Prism software version 10.1.2. Thresholds were: * $p<0.05$; ** $p<0.01$; *** $p<0.001$; $p>0.05$, not significant.

Results

C. clostridioforme LM41 is a poly-lysogen harbouring 15 prophage regions

PHASTER analysis of the LM41 genome revealed 29 predicted prophage regions[18]. These regions were subsequently interrogated to ascertain the presence of classical prophage-associated functional modules to confirm the hits as phage. Prophage completeness was

bioRxiv preprint doi: https://doi.org/10.1101/2024.02.29.582698; this version posted February 29, 2024. The copyright holder for this preprint (which was not certified by peer review) is the author/funder, who has granted bioRxiv a license to display the preprint in perpetuity. It is made available under aCC-BY-NC-ND 4.0 International license.

estimated using Average Amino Acid Identity (AAI) comparison via PhageScope[27], followed by manual inspection to ensure that the regions possessed essential functional modules, with genes arranged in the appropriate direction(s) to enable expression as operons. Using these criteria, 15 prophage regions were identified (Figures 1 and 2; Table 2). The genome organisation, size, and gene synteny of the majority of these prophages is reminiscent of prophages from other Gram positive species, in particular, the siphoviruses of *Staphylococcus aureus*. Four prophages (LM41φ1, φ4, φ10 and φ15) returned completeness scores of 100, suggesting that they are intact, and putatively functional. Interestingly, prophages LM41φ1 and LM41φ4 are highly similar to one another (99.02% ID across 74% of the phage sequence), with divergence occurring principally in the integrase, *cI/cro* lysogeny region, and in the latter half of the replication module.

Prophage regions LM41φ7 and LM41φ9 returned poor completeness scores (<60), suggesting that these are defective phages due to loss of parts of their coding sequence. Indeed, LM41φ7 appears to be a prophage remnant, encoding only lysogeny and replication modules before being interrupted by the integrase of LM41φ8.

Regions LM41φ2, φ8, φ11 and φ14 were classified as 'unknown' on the basis that they returned completeness scores of >60-<100. In addition, though prophages LM41φ3, φ5, φ6, φ12 and φ13 returned completeness scores of 100, manual inspection of their genomes revealed unusual characteristics predicted to affect prophage viability, hence we also categorised them as 'unknown' pending further investigation.

LM41φ3 exhibits peculiarities in its integrase (*orfs1-2*); namely, that *orf2* carries a putative frameshift mutation that results in a premature stop codon after residue P199, splitting the integrase sequence, and likely rendering the prophage defective. Meanwhile, compared to the other prophages, LM41φ5, has an unusual genomic composition, with a larger lysogeny module (*orf1-13*) containing two putative integrase sequences (*orf6-7*) located between proteins comprising a complete type I restriction modification system. In the case of Orf6-7, these putative integrase proteins are smaller than expected for a typical functional integrase (Orf6, 165 aa; Orf7, 167 aa) suggesting that these may be an integrase truncated by mutation.

bioRxiv preprint doi: https://doi.org/10.1101/2024.02.29.582698; this version posted February 29, 2024. The copyright holder for this preprint (which was not certified by peer review) is the author/funder, who has granted bioRxiv a license to display the preprint in perpetuity. It is made available under aCC-BY-NC-ND 4.0 International license.

We attempted to investigate this by searching for related sequences to determine whether a premature stop codon had been introduced by single nucleotide polymorphism to φ5, however a BLASTn search of the sequence encompassing *orf6-7* returned no matches with significant similarity, leaving us unable to resolve this question at this time. φ5 also carries two open reading frames (ORF) predicted to encode recombinases (*orf68-69*) at the terminal end of the prophage sequence. These recombinases are closer in length to that expected for a functional integrase protein (Orf68, 420 aa; Orf69, 282 aa), raising questions as to whether one of these could catalyse the integration of the phage at the *att*B site if indeed the first integrase is non-functional. In addition, we were unable to identify certain components essential for virion packaging in LM41φ5, namely the large terminase subunit and portal protein, raising questions about the capability of this phage to package its genome into procapsids.

LM41φ6 and LM41φ12 exhibit anomalies in their DNA replication and lysis modules, respectively, on account of insertion of a putative group II intron reverse transcriptase/maturase (LM41φ6 *orf20*; LM41φ12, *orf78*). LM41φ6 *orf20* is positioned between two putative DNA helicases (*orf17* and *orf21*). *orf17* and *orf21* are not duplicated genes as they do not display any significant nucleotide similarity. Rather, BLASTn analysis of *orf17* and *orf21* sequences revealed hits with high similarity to the virulence associated protein E (putative DNA helicase) protein from Caudoviricetes sp. isolate ctdym5 [Acc: BK055266] (*orf17*: 99.92% identity, 51% cover, E value 0.0; *orf21*: 99.83% identity, 47% cover, E value 0.0), suggesting that *orfs17* and *21* are one ORF that has been split by the insertion of the putative group II intron. This likely eliminates the functionality of the helicase protein and renders the phage incapable of initiating replication following activation. In LM41φ12, *orf78* is positioned divergently to its flanking genes, potentially affecting transcription of the late module as a polycistronic transcript and therefore affecting the ability of the phage to induce host lysis.

Finally, the data obtained for region φ13 were puzzling. A completeness score of 100 was returned for this 136.5 kb region, suggesting potential functionality, however manual inspection revealed the presence of a variety of prophage sequences with differing levels of completeness. Some of the sequences within region 13 were reminiscent of Mu-type phage,

bioRxiv preprint doi: https://doi.org/10.1101/2024.02.29.582698; this version posted February 29, 2024. The copyright holder for this preprint (which was not certified by peer review) is the author/funder, who has granted bioRxiv a license to display the preprint in perpetuity. It is made available under aCC-BY-NC-ND 4.0 International license.

hence, we divided the 136.5 kb region into sub-regions (α-ε) by matching the predicted functions of the ORFs relative to the functional modules expected for a complete Mu-type phage (i.e. a transposase, ATP-binding or DNA replication protein indicated the likely start of a phage sequence, while a tail or recombinase indicated the likely end). We then refined the regions by searching for hits using BLASTn and assessing completeness using PhageScope (Figure 2).

Regions φ13β, γ and ε returned low completeness scores (49.4, 18.8 and 41.2, respectively), suggesting that these areas are defective phage remnants. The most complete stretches of prophage genome in this region are the 51.0 kb φ13α (*orf1-79,* completeness score 99.65) and 34.2 kb φ13δ (*orf128-192,* completeness score 94.11) regions (Figure 2). Prophage φ13α appears to encode most of the required modules for replication and assembly of phage virions. However, despite encoding two putative integrase genes at its 3' terminus, it lacks a clear lysogeny module and does not encode a Mu transposase C-terminal domain-containing protein to permit transposable replication, suggesting that it may be incomplete. Prophage φ13δ has high similarity to *Clostridium* phage Villandry (BLASTn: 95.82% identity, 96% cover, E value 0.0, Acc ON453902.1) and is reminiscent of the prototypical transposable phage Mu, encoding putative candidates for a repressor (*orf129*), a *ner*-like transcriptional regulator (*orf139*), a Mu transposase (*orf140*), a Mor transcription activator family protein (*orf158*) and structural components such as Mu-like prophage I protein (*orf167*), Phage Mu protein F like protein (*orf166*) and Mu-like prophage major head subunit gpT (*orf169*).

LM41 prophages exhibit diversity in their lysogeny control mechanisms

Our analysis revealed diversity in the lysogeny control mechanisms of the LM41 prophages, with three groups identified: classical λ-like CI/Cro systems[23]; ImmR/ImmA-like systems similar to that used by the *Bacillus subtilis* integrative conjugative element ICE*Bs*1[29]; and systems reminiscent of the CI/Cro-like C/Ner system of *E. coli* phage Mu[30].

Most prophages (10/15) appear to possess lysogeny systems reminiscent of the classical λ-like CI/Cro system. Prophages LM41φ1, φ3, φ4, φ6, φ7, φ9, φ10, φ11, φ14 and

bioRxiv preprint doi: https://doi.org/10.1101/2024.02.29.582698; this version posted February 29, 2024. The copyright holder for this preprint (which was not certified by peer review) is the author/funder, who has granted bioRxiv a license to display the preprint in perpetuity. It is made available under aCC-BY-NC-ND 4.0 International license.

φ15 each possess a pair of adjacent divergently transcribed genes in their putative lysogeny modules, several of which are predicted to be helix-turn-helix transcriptional regulators, representing probable CI-like repressors. Using PhagePromoter[28], we detected divergent promoters in the intergenic region between these ORFs (Figure 2), lending support to our hypothesis that these ORFs encode a CI/Cro-like lysogeny switch in these phages.

Prophages LM41φ2, φ5 and φ12 appear to encode systems analogous to the ImmR/ImmA regulatory systems that have been described for *B. subtilis* ICE*Bs*1[29] and some phage-inducible chromosomal islands in staphylococci[31]. In the lysogeny modules of φ2 and φ12, *orf*4 is predicted to encode an ImmA/IrrE family metallo-endopeptidase which is located directly adjacent to *orf5*. Orf5 is predicted to be a helix-turn-helix (HTH) transcriptional regulator, which we propose to be ImmR-like based on its functional prediction and synteny with *immR* from ICE*Bs*1. Importantly, *orfs4-5* are transcribed in the same direction (leftward), while the downstream ORF (*orf6*), predicted to encode a second HTH transcriptional regulator, is transcribed in the rightward direction towards the DNA replication module. Within the intergenic region between *orf5* and *orf6* in φ2, PhagePromoter predicted the presence of two divergent promoters akin to that observed for P*immR* and P*xis* in ICE*Bs*1 (Figure 2). Conversely, in φ5 and φ12, a pair of convergent promoters were predicted in the intergenic regions between *orfs13-14* (φ5) and *orfs5-6* (φ12), suggesting that transcriptional interference similar to that observed in coliphage 186[32] may play a role in regulating the lysogenic-lytic control switches in these prophages.

The final lysogeny system that we observed is reminiscent of the C/Ner system of *E. coli* phage Mu. In phage Mu, the 197-aa repressor protein (C) is divergently transcribed from the 76-aa DNA binding protein, Ner, which functions to negatively regulate transcription of the replicative transposition genes[30]. LM41φ13 appears to be a highly plastic region on the LM41 chromosome that contains the multiple Mu-type prophage/remnants arranged consecutively, which we have designated φ13α-ε. In LM41φ13, Orf80, located in region φ13β, is predicted to be a 168-aa HTH transcriptional regulator and is transcribed divergently from the downstream gene, *orf*82, which is also predicted to encode a 51-aa HTH transcriptional regulator (BLASTp:

bioRxiv preprint doi: https://doi.org/10.1101/2024.02.29.582698; this version posted February 29, 2024. The copyright holder for this preprint (which was not certified by peer review) is the author/funder, who has granted bioRxiv a license to display the preprint in perpetuity. It is made available under aCC-BY-NC-ND 4.0 International license.

100% identity, 98% cover, E value 1e-26, Acc: WP_303009215.1) (Figure 2). Immediately downstream, *orf*83 is predicted to encode a protein with a Mu transposase C-terminal domain. The similar size, synteny and functional predictions of *orf60*, *orf62 and orf63* from LM41φ13β with that of the genes encoding C, Ner and the transposase from the classical phage Mu, suggests that the functional ancestor of this phage utilised lysogeny regulation mechanism similar to that of phage Mu. A similar arrangement is present in region φ13δ, however 9 ORFs with hypothetical functions are located between the putative *c* (*orf129*) and *ner* (*orf139*) homologs.

LM41 prophages are predicted to be morphologically diverse

Excepting the remnants of φ7, φ13β and φ13γ, genome analysis indicated that all LM41 prophages are tailed, with each of the major tail groups represented (Table 2). Prophages φ1 and φ4 are predicted to carry a single tail gene (*orf61* and *orf63*, respectively). Their products are predicted to be baseplate wedge subunits with homology to tail fibre (spike) proteins, suggesting that these may be podoviruses. Tail sheath proteins were observed in the genomes of φ3, φ8, φ10, φ13δ, φ14 and φ15, suggesting that these may be myoviruses with contractile tails. The remaining prophages, φ2, φ5, φ6, φ9, φ11, φ12, φ13α and φ13ε, possessed tape measure proteins but no sheaths, suggesting that they may be siphoviruses.

Phage particles are spontaneously released from *C. clostridioforme* LM41

We sought to determine whether we could identify any of the phages in the supernatant of LM41 cultures. Treatment with classical SOS-inducers such as mitomycin C, ciprofloxacin and norfloxacin failed to induce lysis of LM41 cultures and did not lead to significantly higher levels of encapsidated phage DNA in induced cultures compared with basal release in untreated cultures (Figure 3), suggesting that these chemicals are not potent inducers of LM41 prophages under the conditions tested.

Using a dual approach, we examined the profile of phages released following spontaneous induction for our subsequent experiments. Firstly, qPCR was used to identify the

bioRxiv preprint doi: https://doi.org/10.1101/2024.02.29.582698; this version posted February 29, 2024. The copyright holder for this preprint (which was not certified by peer review) is the author/funder, who has granted bioRxiv a license to display the preprint in perpetuity. It is made available under aCC-BY-NC-ND 4.0 International license.

presence of encapsidated DNA (indicative of phage) in LM41 culture supernatants. Briefly, filtered supernatants were divided into duplicate samples, of which one was DNase treated and the other was kept as an untreated control. DNase treatment enabled differentiation of encapsidated phage DNA, which is protected from degradation by the phage protein capsid, from DNA present in the sample that has been released from lysed bacterial cells. For all targets, DNase treatment reduced the quantity of DNA present in the sample (Figure 4A). Following treatment, levels of the bacterial small ribosomal subunit protein 10 (*s10p*) housekeeper gene were reduced below the respective no template control (NTC), suggesting comprehensive degradation of bacterial DNA in the sample. In contrast, excepting φ13ε, each of the phage targets remained detectable relative to their respective NTCs, suggesting the presence of phage particles in the supernatant, albeit often at extremely low levels. The differences in mean Cq values between treated and untreated samples were lowest for φ1 (5.11), φ4 (8.06), φ2 (8.37) and φ10 (8.69), suggesting that these phages were most abundant. Indeed, quantification of the levels of each phage in the sample relative to the *s10p* housekeeper was performed using the $2^{-\Delta\Delta Ct}$ method and showed that φ1 was the most abundant phage in the sample (mean ± SD: 28.45 ± 23.35), followed by φ4 (2.95 ± 0.72), φ2 (2.90 ± 1.99) and φ10 (1.87 ± 0.26) (Figure 4B).

To visualise the phage particles spontaneously released into the culture supernatant, we DNase treated filtered culture supernatants of LM41, then NaCl-PEG 8000 precipitated the phage capsids, which were subsequently imaged using negative staining and transmission electron microscopy (TEM). Icosahedral particles with diameters in the range 64-67 nm were observed (Figure 5A&B), which is consistent with the dimensions of staphylococcal phages with similar genome sizes[33]. We also observed one example of a smaller-sized capsid, with a diameter of 39.4 nm (Figure 5C). Some virion particles appeared to have short protrusions (~7-8 nm length) emanating from the capsid, raising the possibility that they are podoviruses (Figures 5A). The other structures observed were consistent with siphovirus or myovirus morphology, with the smaller diameter particle associated with what appears to be a large tail structure approximately 78.8 nm in length and 22.8 nm wide (Figure 5C). Though it is

bioRxiv preprint doi: https://doi.org/10.1101/2024.02.29.582698; this version posted February 29, 2024. The copyright holder for this preprint (which was not certified by peer review) is the author/funder, who has granted bioRxiv a license to display the preprint in perpetuity. It is made available under aCC-BY-NC-ND 4.0 International license.

401 impossible to determine from the imaging analysis which LM41 phages are present in the
402 sample, it is likely that the majority of the podovirus-like particles observed are LM41φ1 given
403 that our previous experiment indicated that φ1 is the most abundant phage and is predicted
404 to have podovirus morphology.
405
406 **Accessory genes**
407 We next sought to determine whether there was an obvious advantage to LM41 in maintaining
408 so many prophage sequences. Bacteriophages often carry accessory genes that do not
409 directly contribute to the lysogenic lifecycle but that may provide a benefit to the host bacterium
410 by altering its phenotype in a process known as lysogenic conversion[34]. Importantly, accessory
411 genes may also be retained as part of cryptic (defective) prophages[35]. We examined LM41φ1-
412 15 for the presence of accessory genes that may confer some sort of benefit to the LM41 host
413 cell. No products classically associated with bacterial morons ('more-on's), such as exotoxins
414 or immune-evasion factors, were observed in any of the prophages encoded by LM41. This
415 was not necessarily surprising, as *C. clostridioforme* is a member of the healthy gut microbiota
416 and is not considered to be virulent. It should, however, be stated that many of the putative
417 ORFs encoded by these prophages are predicted to be hypothetical proteins, so the presence
418 of such factors cannot be definitively ruled out. We did note the presence of several potentially
419 interesting proteins which can be broadly grouped as: restriction-modification (RM) system
420 components; diversity-generating elements; hypothetical proteins with some similarity to large
421 polyvalent proteins; phage defence factors; anti-phage defence factors; and proteins with
422 possible roles in adaptation within the host intestine (Table 3).
423 Proteins with roles in Type I RM were identified in LM41φ5, LM41φ13β and LM41φ13ε.
424 Prophage LM41φ5 encodes a complete Type I RM system, encompassing three specificity
425 subunits (*hsd*S), a DNA methyltransferase and a restriction subunit. LM41φ13β also encodes
426 a complete Type I RM system comprising of HsdM (SAM-dependent DNA methyltransferase),
427 HsdS (specificity subunit), and HsdR (endonuclease subunit R), where subunits HsdM and
428 HsdR have high homology with similar proteins in *Ruminococcus sp.* (both 97.31% identity),

bioRxiv preprint doi: https://doi.org/10.1101/2024.02.29.582698; this version posted February 29, 2024. The copyright holder for this preprint (which was not certified by peer review) is the author/funder, who has granted bioRxiv a license to display the preprint in perpetuity. It is made available under aCC-BY-NC-ND 4.0 International license.

while HsdS shares some similarity with a protein from *Anaerosporobacter faecicola* (60.22% identity). Interestingly, we also identified an ORF predicted to have limited similarity (61.11% identity) to the *E. coli* restriction alleviation protein, Lar (also known as RalR), in LM41φ10. Lar functions to modulate the activity of the *E. coli* K-12 host RM systems in order to protect the Rac prophage from destruction[36].

In addition to the RM systems, we also noted the presence of a number of other factors associated with potential phage defence and anti-phage defence systems. Multiple different Toxin-Antitoxin (TA) systems were associated with the LM41 prophages: a HicB/HicA-type system identified in LM41φ10; a RelB/RelE-type system in LM41φ13α; and a SymE-like type I toxin in both LM41φ5 and LM41φ13α. Amidoligase enzymes were also identified in prophages φ5 and φ13α. In terms of anti-phage defence systems, anti-CRISPR systems were identified in φ1, φ2 and φ9, while a predicted TA system antitoxin was observed in φ13δ.

The presence of diversity-generating elements was also noted in multiple LM41 prophages. Group II intron reverse transcriptase/maturase proteins were identified in prophages LM41φ2 (Orf51), LM41φ6 (Orf20), and LM41φ12 (Orf78), while LM41φ3 is predicted to carry both a reverse transcriptase/maturase family protein (Orf76) and a homolog of *Bordetella* phage BPP-1 diversity-generating retroelement protein Avd (Orf73), which in BPP-1 facilitates sequence variation in target protein genes, enabling changes in host cell surface factors[37,38].

Proteins with potential roles in influencing adaptation of the bacterial lysogen within the host intestinal environment were also observed. These include Orf60 of LM41φ8 and Orf149 of LM41φ9, which encode putative haemolysins, and factors influencing host metabolism, such as a gamma-glutamyl cyclotransferases in φ13α and φ13ε, an ORF with dextransucrase activity in φ1, and phosphoadenosine phosphosulfate reductases in φ13δ and φ14.

Finally, prophages LM41φ1 and LM41φ4 encode an unusually large (8 kb) ORF at their 3' ends, which constitutes almost 20% of the phage genome sequence. Both ORFs are predicted to be hypothetical proteins, but have some limited similarity (53.84% ID) to large

bioRxiv preprint doi: https://doi.org/10.1101/2024.02.29.582698; this version posted February 29, 2024. The copyright holder for this preprint (which was not certified by peer review) is the author/funder, who has granted bioRxiv a license to display the preprint in perpetuity. It is made available under aCC-BY-NC-ND 4.0 International license.

polyvalent protein-associated domain 3 from *Podoviridae* sp., suggesting that they could play a role in protecting and establishing the phage DNA when it enters a new host cell[39].

Discussion

C. clostridioforme LM41 has an atypically large genome for this species, with a strikingly high proportion of DNA attributed to mobile genetic elements[18]. This work sought to characterise the prophage sequences associated with this strain to determine whether they might contribute to its enhanced fitness in the dysbiotic gut. Interrogation of the LM41 genome sequence revealed poly-lysogeny: 15 prophage-derived sequences – comprising >9.6% of the bacterium's 7.78 Mb genome – were observed, many with genomic organisation and size reminiscent of the well-characterised Gram positive staphylococcal siphovirus phages[40]. Four of the LM41 phages are predicted to encode all of the necessary modules for functionality, with a further nine phages requiring additional characterisation. We attempted to test functionality of the LM41 prophages experimentally using chemical induction, however the classical SOS-inducing antibiotics mitomycin C, norfloxacin and ciprofloxacin failed to induce bacterial lysis or significantly increase the quantity of encapsidated DNA released from LM41 compared to the untreated control, suggesting that LM41 prophages do not respond efficiently to this type of inducing signal. This observation is not necessarily surprising as work in *Clostridioides difficile* has shown that some prophages respond more effectively to fluoroquinolone antibiotic exposure than to the 'gold-standard' mitomycin C[41]. Furthermore, others have shown that in a variety of species of human gut bacteria, fewer than one quarter of prophages predicted to be functional using bioinformatics could be induced under experimental conditions[42]. This may suggest higher than expected rates of cryptic phage carriage in these bacteria or could mean that prophages in these species have different inducing signals to those from classically studied hosts such as *E. coli* and *S. aureus*. Arguably, it is likely that other prophage inducing signals occur in the gut environment given the lack of potent DNA damaging agents typically present in physiological habitats, and recent work has shown that in *Vibrio spp*., prophage-encoded transcription factors can activate small proteins

bioRxiv preprint doi: https://doi.org/10.1101/2024.02.29.582698; this version posted February 29, 2024. The copyright holder for this preprint (which was not certified by peer review) is the author/funder, who has granted bioRxiv a license to display the preprint in perpetuity. It is made available under aCC-BY-NC-ND 4.0 International license.

485 which induce their prophage in an SOS-independent manner[43], while *S. aureus* prophage
486 phiMBL3 can be induced independently of the SOS response by a pyocyanin metabolite from
487 *Pseudomonas aeruginosa*[44]. Accordingly, further work is necessary to screen a variety of
488 inducing agents against LM41 prophages before they can be conclusively determined to be
489 functional or defective.

490 Within lysogenic populations, spontaneous prophage induction can occur in a small
491 proportion of cells, leading to release of low titres of phage into the surrounding environment[45].
492 Molecular examination of LM41 culture supernatants confirmed that LM41φ1, φ4 and φ10
493 particles are spontaneously released, supporting our prediction of these prophages as
494 functional. φ2 was also detected, suggesting that this phage is functional despite scoring <100
495 for completeness. TEM imaging showed that spontaneously produced particles are
496 predominantly podoviruses, though observation of other putative phage particles with longer
497 tails indicates diversity in the morphological characteristics of LM41 phages. We also observed
498 diversity among the lysogeny control systems utilised by the different prophages, suggesting
499 the existence of a diverse community of phages within the *Lachnospiraceae* that can employ
500 different mechanisms in order to maintain their latent state within their host bacterium.

501 Three regions were also observed that contained phage remnants to varying degrees,
502 with the defects present predicted to abolish the ability of these phages to excise, replicate,
503 and/or package efficiently. LM41φ13 was revealed to be not just one phage, but a 136 kb
504 region of phage remnants, presumably derived from excessive or uncontrolled recombination
505 events. A similar Mu-type phage is present in the *C. clostridioforme* LM41 relative
506 *Lachnoclostridium* sp. YL32 (Accession: CP015399), where two copies of the 35.8 kb phage
507 sequence are arranged divergently at genome locations 3,363,626-3,399,467 bp and
508 3,591,511-3,627,351 bp, with each of these sequences displaying high similarity (95.82% ID,
509 89% cover, E-value 0.0) to the δ region of LM41φ13, suggesting the potential for a common
510 ancestor. It is unclear as to how and why the LM41φ13 region became so variable in LM41.
511 In contrast to many well-characterised lysogenic phages, transposable phages do not excise
512 out of the chromosome in order to proliferate[46]. In the case of the archetypal phage Mu, the

bioRxiv preprint doi: https://doi.org/10.1101/2024.02.29.582698; this version posted February 29, 2024. The copyright holder for this preprint (which was not certified by peer review) is the author/funder, who has granted bioRxiv a license to display the preprint in perpetuity. It is made available under aCC-BY-NC-ND 4.0 International license.

integrated phage replicates by looping the bacterial chromosome and cleaving the DNA, enabling the formation of Shapiro intermediate structures whereby the prophage sequence is duplicated and integrated into new sites on the bacterial chromosome at random, in a mechanism similar to a transposon[46]. We can see no obvious explanation for the hypervariability observed in region LM41φ13, however, given the apparent propensity for DNA acquisition by strain LM41, it is possible that this strain has lost some of the mechanisms required for maintaining fidelity in DNA recombination and repair, resulting in the loss of intact phage regions. Additional work will be required to evaluate this theory further.

Given the quantity of prophage DNA carried by LM41, we hypothesised that one or more of the resident prophages contributes to the fitness of the host bacteria in the dysbiotic intestine. Examination of the prophage sequences for the presence of morons (accessory genes with functions not linked to lysogeny) revealed no obvious candidates for the enhanced fitness displayed by LM41 in the gut environment. We did, however, find that the LM41 prophages carry a number of potentially interesting genes, including those with roles in phage defence and anti-phage defence. Defence systems include a variety of DNA methyltransferases, a number of specificity subunits, and two complete Type I RM systems for the modification of DNA, presumably to aid phage defence against degradation by the host bacterium's RM systems. Plasmid carriage of orphan HsdS (specificity) subunits that can interact with chromosomally-encoded HsdM (methylation) and HsdR (restriction) subunits has been described in *Lactococcus lactis*, creating a molecular expansion pack for the host cell Type I RM repertoire without requiring carriage of a full HsdMSR system[47]. It is tempting to speculate that a similar combinational system utilising phage-encoded specificity or methyltransferase subunits with native restriction and/or methylation components may contribute to the ability of LM41 to accept foreign DNA if it can be recognised and methylated by these enzymes prior to destruction by the host cell's restriction systems, possibly lending some explanation as to why this strain appears to have gained so much horizontally-acquired DNA compared to its most closely related strains. Further to this, we observed a protein in LM41φ10 with limited similarity to the *E. coli* restriction alleviation protein, Lar, which has a

bioRxiv preprint doi: https://doi.org/10.1101/2024.02.29.582698; this version posted February 29, 2024. The copyright holder for this preprint (which was not certified by peer review) is the author/funder, who has granted bioRxiv a license to display the preprint in perpetuity. It is made available under aCC-BY-NC-ND 4.0 International license.

role in modulating the activity of *E. coli*-encoded RM systems to protect prophage DNA[36]. It is not impossible that the Lar-like protein of LM41φ10 exerts global impacts upon its host organism, and that this could function synergistically with the other phage-encoded RM components to retain foreign DNA in LM41. In order to test this theory, a phage-cured strain of LM41 would need to be generated, and its ability to accept exogenous DNA compared with the parental LM41 and with variants carrying defined combinations of prophages. Unfortunately, given the paucity of genetic tools to permit manipulation of this organism, such experiments are not currently possible.

Other putative defence systems include TA systems, which can facilitate phage defence at the population level, inducing processes such as abortive infection following infection of the host cell or by inhibiting virion formation[48,49]. We also observed factors with roles in modifying the host cell surface to prevent superinfection of lysogens, potentially acting similarly to the amidoligase of *E. coli* phage phiEco32 which modifies cell wall receptors to prevent adsorption by competing phages[50]. As bacteria and their phages are engaged in a constant arms race, evolution of anti-phage defence systems on the part of the phage is necessary to overcome bacterial defences. LM41 prophages encode anti-CRISPR proteins and carry solitary TA system antitoxin components with potential roles in subverting phage defence systems. It is currently unclear whether these antitoxins are part of degenerate TA systems or whether these proteins could act as anti-phage defence systems by enabling the phages to counter toxins from other host- or phage-encoded TA systems.

Group II reverse transcriptase/maturase proteins were also detected in a number of prophages. The role of these proteins for phage or host cell biology is unclear. Indeed, it is possible that these elements have been acquired elsewhere and have become integrated within the prophage sequences, as seems likely in the case of LM41φ6 where the putative helicase ORF has been interrupted by the insertion of a putative group II reverse transcriptase/maturase protein. This hypothesis is further supported by the fact that 29 LtrA group II intron sequences are present throughout the LM41 genome, suggesting that these are a feature of the host rather than the phages.

bioRxiv preprint doi: https://doi.org/10.1101/2024.02.29.582698; this version posted February 29, 2024. The copyright holder for this preprint (which was not certified by peer review) is the author/funder, who has granted bioRxiv a license to display the preprint in perpetuity. It is made available under aCC-BY-NC-ND 4.0 International license.

Finally, we detected two putative haemolysin proteins carried by prophages φ8 and φ9. It is possible that these are misannotations, as φ9 Orf149 shows high homology to CHAP domain-containing protein from *Enterocloster sp.* (BLASTp: 99% query cover, E-value 0.0, 98.45% ID to accession WP_256170368.1) which is predicted to have a role in peptidoglycan hydrolysis, suggesting a role in phage-mediated cell lysis. However, if these proteins are indeed haemolysins, they could potentially provide LM41 with an advantage in the gut, perhaps by scavenging iron from the host via haemolysis. The ability of LM41 to lyse erythrocytes could be evaluated *in vitro* to examine whether LM41 has the potential to participate in nutrient acquisition in this way.

Phages are the most numerous entities within the gut microbiome[51], and yet the phages associated with members of the microbiota remain poorly characterised. Here, we have identified an interesting example of poly-lysogeny in *C. clostridioforme* strain LM41 and have utilised bioinformatic tools and experimental approaches to offer insight into some of the characteristics of these phages, shedding light on their potential impact upon their host bacterium.

Conflicts of interest

The authors declare no competing interests.

Funding information

S.H. and D.W. are supported by funding from Tenovus Scotland, grant number S23-16. K.T. is supported by UKRI Biotechnology and Biosciences Research Council (BBSRC) grant number BB/V001876/1 to D.M.W.

Author contributions

S.H. and D.W. designed the study and obtained funding. S.H. wrote the manuscript. S.H. and A.M. performed the experiments. S.H., A.M. and D.W. performed the analysis. K.T. assisted

bioRxiv preprint doi: https://doi.org/10.1101/2024.02.29.582698; this version posted February 29, 2024. The copyright holder for this preprint (which was not certified by peer review) is the author/funder, who has granted bioRxiv a license to display the preprint in perpetuity. It is made available under aCC-BY-NC-ND 4.0 International license.

596 with experiments and performed the statistical analysis. M.M. prepared the samples and
597 performed TEM imaging.
598
599 **Acknowledgements**
600 The authors thank Ester Serrano for helpful advice and assistance in preparing phage samples
601 for TEM.
602
603 **References**
604 1. Krajmalnik-Brown, R., Ilhan, Z.-E., Kang, D.-W. & Dibaise, J. K. Effects of Gut
605 Microbes on Nutrient Absorption and Energy Regulation. *Nutr Clin Pr.* **27**, 201–214
606 (2012).
607 2. Mazmanian, S. K., Liu, C. H., Tzianabos, A. O. & Kasper, D. L. An Immunomodulatory
608 Molecule of Symbiotic Bacteria Directs Maturation of the Host Immune System. *Cell*
609 **122**, 107–118 (2005).
610 3. Yano, J. M. *et al.* Indigenous Bacteria from the Gut Microbiota Regulate Host
611 Serotonin Biosynthesis Article Indigenous Bacteria from the Gut Microbiota Regulate
612 Host Serotonin Biosynthesis. doi:10.1016/j.cell.2015.02.047
613 4. Barrett, E., Ross, R. P., O'Toole, P. W., Fitzgerald, G. F. & Stanton, C. γ-Aminobutyric
614 acid production by culturable bacteria from the human intestine. *J. Appl. Microbiol.*
615 **113**, 411–417 (2012).
616 5. Bansal, T., Alaniz, R. C., Wood, T. K. & Jayaraman, A. The bacterial signal indole
617 increases epithelial-cell tight-junction resistance and attenuates indicators of
618 inflammation. doi:10.1073/pnas.0906112107
619 6. Khosravi, A. & Mazmanian, S. K. Disruption of the gut microbiome as a risk factor for
620 microbial infections. *Current Opinion in Microbiology* **16**, (2013).
621 7. Goodrich, J. K. *et al.* Human genetics shape the gut microbiome. *Cell* **159**, (2014).
622 8. Dethlefsen, L. & Relman, D. A. Incomplete recovery and individualized responses of
623 the human distal gut microbiota to repeated antibiotic perturbation. *Proc. Natl. Acad.*

bioRxiv preprint doi: https://doi.org/10.1101/2024.02.29.582698; this version posted February 29, 2024. The copyright holder for this preprint (which was not certified by peer review) is the author/funder, who has granted bioRxiv a license to display the preprint in perpetuity. It is made available under aCC-BY-NC-ND 4.0 International license.

Sci. U. S. A. **108**, (2011).

9. Hildebrandt, M. A. *et al.* High-Fat Diet Determines the Composition of the Murine Gut Microbiome Independently of Obesity. *Gastroenterology* **137**, (2009).

10. Joossens, M. *et al.* Dysbiosis of the faecal microbiota in patients with Crohn's disease and their unaffected relatives. *Gut* **60**, (2011).

11. Ley, R. E. *et al.* Obesity alters gut microbial ecology. *Proc. Natl. Acad. Sci. U. S. A.* **102**, (2005).

12. Wang, J. *et al.* A metagenome-wide association study of gut microbiota in type 2 diabetes. *Nature* **490**, 55–60 (2012).

13. Karlsson, F. H. *et al.* Gut metagenome in European women with normal, impaired and diabetic glucose control. *Nature* **498**, 99–103 (2013).

14. Qin, J. *et al.* A metagenome-wide association study of gut microbiota in type 2 diabetes. *Nat. 2012 4907418* **490**, 55–60 (2012).

15. Finegold, S. M. *et al.* Gastrointestinal microflora studies in late-onset autism. *Clin. Infect. Dis.* **35**, (2002).

16. Le Chatelier, E. *et al.* Richness of human gut microbiome correlates with metabolic markers. *Nature* **500**, 28 (2013).

17. Raymond, F. *et al.* The initial state of the human gut microbiome determines its reshaping by antibiotics. *ISME J.* **10**, 707–720 (2016).

18. Kamat, M. T. *et al.* Genomic diversity of novel strains of mammalian gut microbiome derived Clostridium XIVa strains is driven by mobile genetic element acquisition. *bioRxiv* 2024.01.22.576618 (2024). doi:10.1101/2024.01.22.576618

19. Carding, S. R., Davis, N. & Hoyles, L. Review article: the human intestinal virome in health and disease. *Aliment. Pharmacol. Ther.* **46**, 800–815 (2017).

20. Brüssow, H., Canchaya, C. & Hardt, W.-D. Phages and the Evolution of Bacterial Pathogens: from Genomic Rearrangements to Lysogenic Conversion. *Microbiol. Mol. Biol. Rev.* **68**, 560 (2004).

21. Novick, R. P. & Ram, G. Staphylococcal pathogenicity islands — movers and shakers

bioRxiv preprint doi: https://doi.org/10.1101/2024.02.29.582698; this version posted February 29, 2024. The copyright holder for this preprint (which was not certified by peer review) is the author/funder, who has granted bioRxiv a license to display the preprint in perpetuity. It is made available under aCC-BY-NC-ND 4.0 International license.

in the genomic firmament. *Current Opinion in Microbiology* (2017). doi:10.1016/j.mib.2017.08.001

22. Cumby, N., Edwards, A. M., Davidson, A. R. & Maxwell, K. L. The Bacteriophage HK97 gp15 Moron Element Encodes a Novel Superinfection Exclusion Protein. *J. Bacteriol.* **194**, 5012 (2012).
23. Casjens, S. R. & Hendrix, R. W. Bacteriophage lambda: Early pioneer and still relevant. *Virology* **479**–**480**, 310–330 (2015).
24. Fillol-Salom, A. *et al.* Bacteriophages benefit from generalized transduction. *PLOS Pathog.* (2019). doi:10.1371/journal.ppat.1007888
25. Arndt, D. *et al.* PHASTER: a better, faster version of the PHAST phage search tool. *Nucleic Acids Res.* **44**, W16–W21 (2016).
26. Bouras, G. *et al.* Pharokka: a fast scalable bacteriophage annotation tool. *Bioinformatics* **39**, (2023).
27. Wang, R. H. *et al.* PhageScope: a well-annotated bacteriophage database with automatic analyses and visualizations. *Nucleic Acids Res.* **52**, D756–D761 (2024).
28. Sampaio, M., Rocha, M., Oliveira, H. & DIas, O. Predicting promoters in phage genomes using PhagePromoter. *Bioinformatics* **35**, 5301–5302 (2019).
29. Bose, B., Auchtung, J. M., Lee, C. A. & Grossman, A. D. A conserved anti-repressor controls horizontal gene transfer by proteolysis. *Mol. Microbiol.* **70**, 570–582 (2008).
30. Goosen, N. & Van de Putte, P. Role of ner protein in bacteriophage Mu transposition. *J. Bacteriol.* **167**, 503–507 (1986).
31. Haag, A. F. *et al.* A regulatory cascade controls Staphylococcus aureus pathogenicity island activation. *Nat. Microbiol. 2021 610* **6**, 1300–1308 (2021).
32. Callen, B. P., Shearwin, K. E. & Egan, J. B. Transcriptional interference between convergent promoters caused by elongation over the promoter. *Mol. Cell* **14**, 647–656 (2004).
33. Spilman, M. S. *et al.* A conformational switch involved in maturation of staphylococcus aureus bacteriophage 80α capsids. *J. Mol. Biol.* **405**, (2011).

bioRxiv preprint doi: https://doi.org/10.1101/2024.02.29.582698; this version posted February 29, 2024. The copyright holder for this preprint (which was not certified by peer review) is the author/funder, who has granted bioRxiv a license to display the preprint in perpetuity. It is made available under aCC-BY-NC-ND 4.0 International license.

680 34. Cumby, N., Davidson, A. R. & Maxwell, K. L. The moron comes of age. *Bacteriophage*
681 **2**, 225 (2012).
682 35. Wang, X. *et al.* Cryptic prophages help bacteria cope with adverse environments. *Nat.*
683 *Commun.* **1**, 147 (2010).
684 36. King, G. & Murray, N. E. Restriction alleviation and modification enhancement by the
685 Rac prophage of Escherichia coli K-12. *Mol. Microbiol.* **16**, 769–777 (1995).
686 37. Alayyoubi, M. *et al.* Structure of the essential diversity-generating retroelement protein
687 bAvd and its functionally important interaction with reverse transcriptase. *Structure* **21**,
688 266–276 (2013).
689 38. Liu, M. *et al.* Reverse transcriptase-mediated tropism switching in Bordetella
690 bacteriophage. *Science (80-.).* **295**, 2091–2094 (2002).
691 39. Iyer, L. M. *et al.* Polyvalent Proteins, a Pervasive Theme in the Intergenomic
692 Biological Conflicts of Bacteriophages and Conjugative Elements. *jb.asm.org 1 J.*
693 *Bacteriol. Downloaded* **199**, 245–262 (2017).
694 40. Xia, G. & Wolz, C. Phages of Staphylococcus aureus and their impact on host
695 evolution. *Infect. Genet. Evol.* **21**, 593–601 (2014).
696 41. Nale, J. Y. *et al.* Diverse temperate bacteriophage carriage in Clostridium difficile 027
697 strains. *PLoS One* **7**, (2012).
698 42. Dahlman, S. *et al.* Temperate gut phages are prevalent, diverse, and predominantly
699 inactive. *bioRxiv* 2023.08.17.553642 (2023). doi:10.1101/2023.08.17.553642
700 43. Silpe, J. E. *et al.* Small protein modules dictate prophage fates during polylysogeny.
701 *Nature* **620**, (2023).
702 44. Jancheva, M. & Böttcher, T. A Metabolite of Pseudomonas Triggers Prophage-
703 Selective Lysogenic to Lytic Conversion in Staphylococcus aureus. *J. Am. Chem.*
704 *Soc.* **143**, (2021).
705 45. Nanda, A. M., Thormann, K. & Frunzke, J. Impact of spontaneous prophage induction
706 on the fitness of bacterial populations and host-microbe interactions. *Journal of*
707 *Bacteriology* **197**, (2015).

bioRxiv preprint doi: https://doi.org/10.1101/2024.02.29.582698; this version posted February 29, 2024. The copyright holder for this preprint (which was not certified by peer review) is the author/funder, who has granted bioRxiv a license to display the preprint in perpetuity. It is made available under aCC-BY-NC-ND 4.0 International license.

46. Harshey, R. M. Transposable phage Mu. *Microbiol. Spectr.* **2**, (2014).

47. Schouler, C., Gautier, M., Ehrlich, S. D. & Chopin, M. C. Combinational variation of restriction modification specificities in Lactococcus lactis. *Mol. Microbiol.* **28**, 169–178 (1998).

48. Guegler, C. K. & Laub, M. T. Shutoff of host transcription triggers a toxin-antitoxin system to cleave phage RNA and abort infection. *Mol. Cell* **81**, 2361-2373.e9 (2021).

49. Kelly, A., Arrowsmith, T. J., Went, S. C. & Blower, T. R. Toxin–antitoxin systems as mediators of phage defence and the implications for abortive infection. *Curr. Opin. Microbiol.* **73**, 102293 (2023).

50. Iyer, L. M., Abhiman, S., Maxwell Burroughs, A. & Aravind, L. Amidoligases with ATP-grasp, glutamine synthetase-like and acetyltransferase-like domains: synthesis of novel metabolites and peptide modifications of proteins. *Mol. Biosyst.* **5**, 1636–1660 (2009).

51. Shkoporov, A. N. & Hill, C. Bacteriophages of the Human Gut: The ‘Known Unknown’ of the Microbiome. *Cell Host Microbe* **25**, 195–209 (2019).

bioRxiv preprint doi: https://doi.org/10.1101/2024.02.29.582698; this version posted February 29, 2024. The copyright holder for this preprint (which was not certified by peer review) is the author/funder, who has granted bioRxiv a license to display the preprint in perpetuity. It is made available under aCC-BY-NC-ND 4.0 International license.

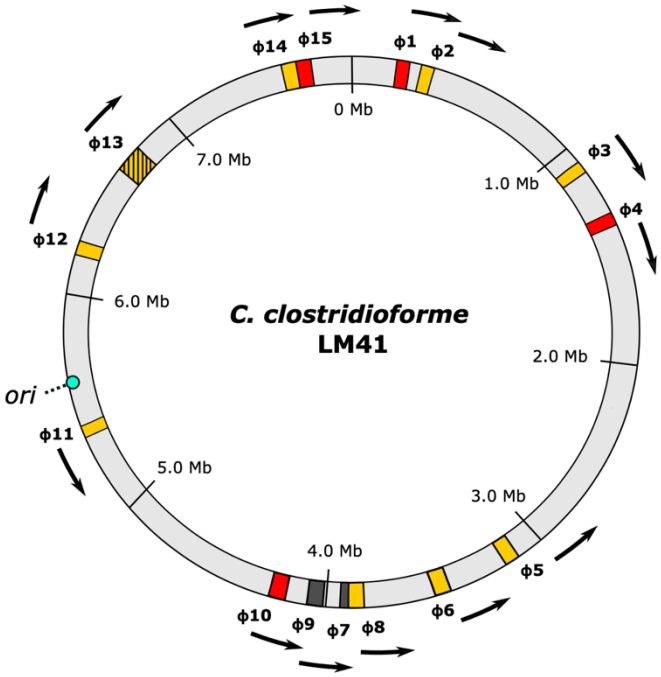

Prophage Region	PhageScope Analysis		Manual inspection comments	Prediction
	CheckV assessment	CheckV completeness		
1	High-quality	100		Functional
2	High-quality	98.86	Truncated integrase sequence (*orf1*)	Unknown
3	High-quality	100	Disrupted integrase (*orf1-2*)	Unknown
4	High-quality	100		Functional
5	High-quality	100	Unusual genome architecture	Unknown
6	High-quality	100	Insertion of group II intron RT into DNA helicase	Unknown
7	Low-quality	27.05	Remnant	Defective
8	Medium quality	62.23	Unusual genome architecture	Unknown
9	Low-quality	46.03		Defective
10	High-quality	100		Functional
11	High-quality	93.12		Unknown
12	High-quality	100		Unknown
13	High-quality	100	Recombination hotspot - contains multiple prophage sequences	Unknown (α, δ)/ Defective (β, γ, ε)
14	Medium-quality	87.93		Unknown
15	High-quality	100		Functional

Figure 1: Arrangement of prophages in the *C. clostridioforme* LM41 chromosome. Locations of each of the prophage regions were mapped according to their coordinates in the LM41 chromosome. Coloured areas indicate the presence of prophages predicted to be functional (red), defective (black), or unknown (yellow) using PhageScope genome completeness assessment followed by manual inspection. Region 13 (hatched) is a putative hot-spot for phage recombination and is predicted to contain multiple phage sequences, some of which are defective remnants and some which are functionally unclassified. Arrows indicate the predicted direction of phage packaging. The bacterial chromosome origin of replication (*ori*) is indicated by the turquoise circle. Image generated using Inkscape v.1

bioRxiv preprint doi: https://doi.org/10.1101/2024.02.29.582698; this version posted February 29, 2024. The copyright holder for this preprint (which was not certified by peer review) is the author/funder, who has granted bioRxiv a license to display the preprint in perpetuity. It is made available under aCC-BY-NC-ND 4.0 International license.

740

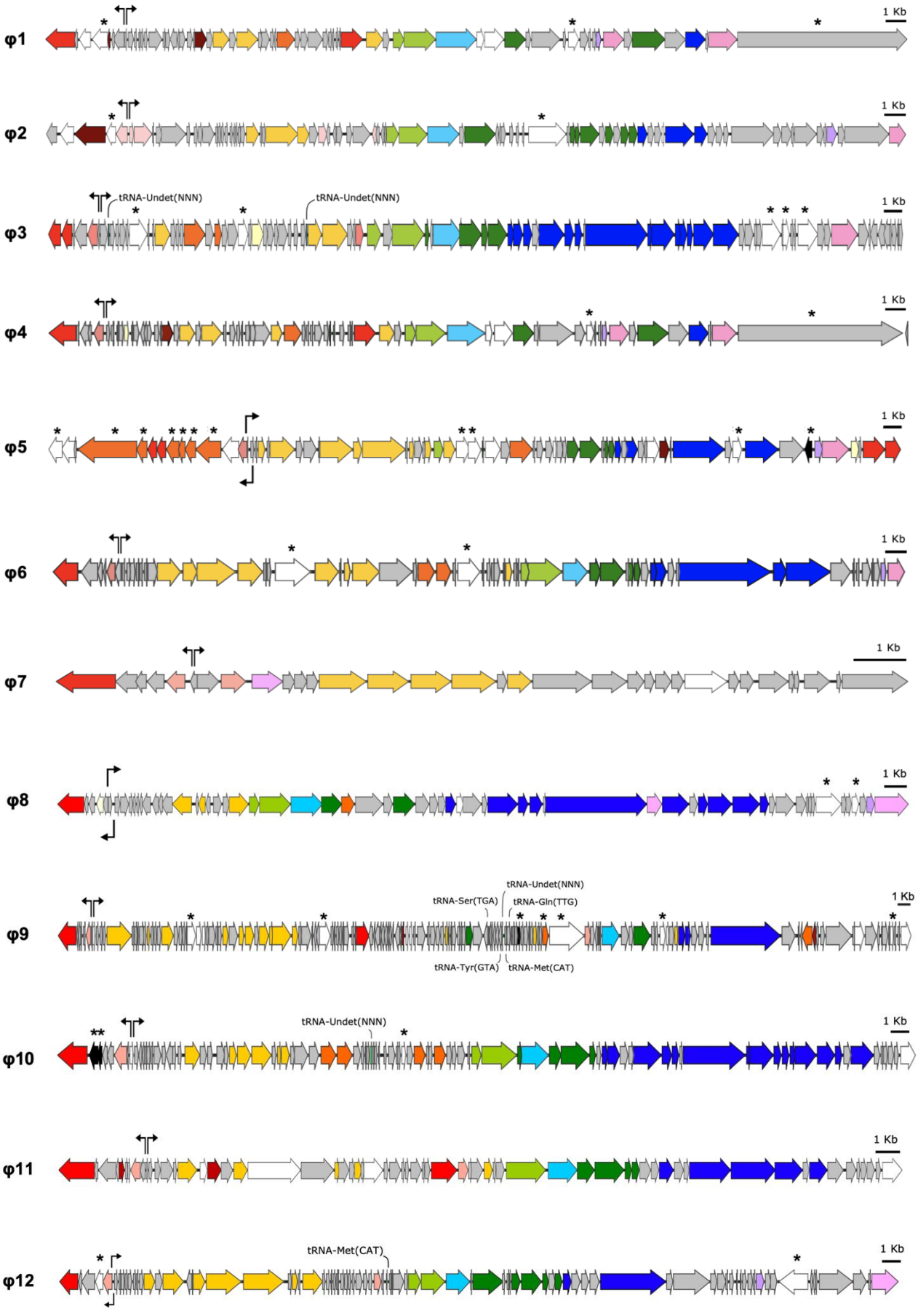

bioRxiv preprint doi: https://doi.org/10.1101/2024.02.29.582698; this version posted February 29, 2024. The copyright holder for this preprint (which was not certified by peer review) is the author/funder, who has granted bioRxiv a license to display the preprint in perpetuity. It is made available under aCC-BY-NC-ND 4.0 International license.

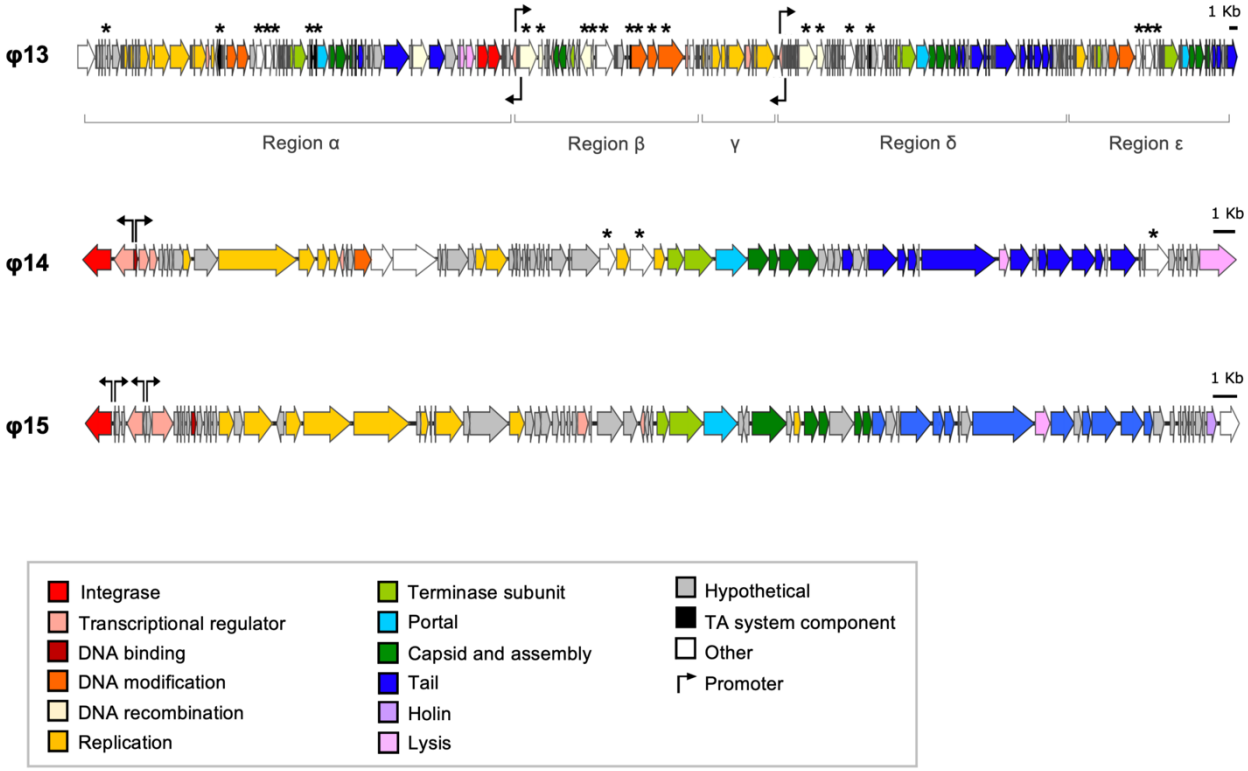

741

742

743 **Figure 2: Genome maps of LM41φ1-15.** Schematic maps of the ORFs predicted for each of
744 the prophage regions identified in *C. clostridioforme* LM41. Genes are coloured according to
745 their predicted functional group with tRNAs indicated. Putative promoters associated with
746 lysogeny control, identified using PhagePromoter, are indicated by black arrows. Asterisks
747 denote the presence of potential accessory genes of interest. 1 Kb scale is denoted by the
748 black bars. Images were generated using Snapgene v.6.1.1 and InkScape v.1 software.

749

750

751

752

753

754

bioRxiv preprint doi: https://doi.org/10.1101/2024.02.29.582698; this version posted February 29, 2024. The copyright holder for this preprint (which was not certified by peer review) is the author/funder, who has granted bioRxiv a license to display the preprint in perpetuity. It is made available under aCC-BY-NC-ND 4.0 International license.

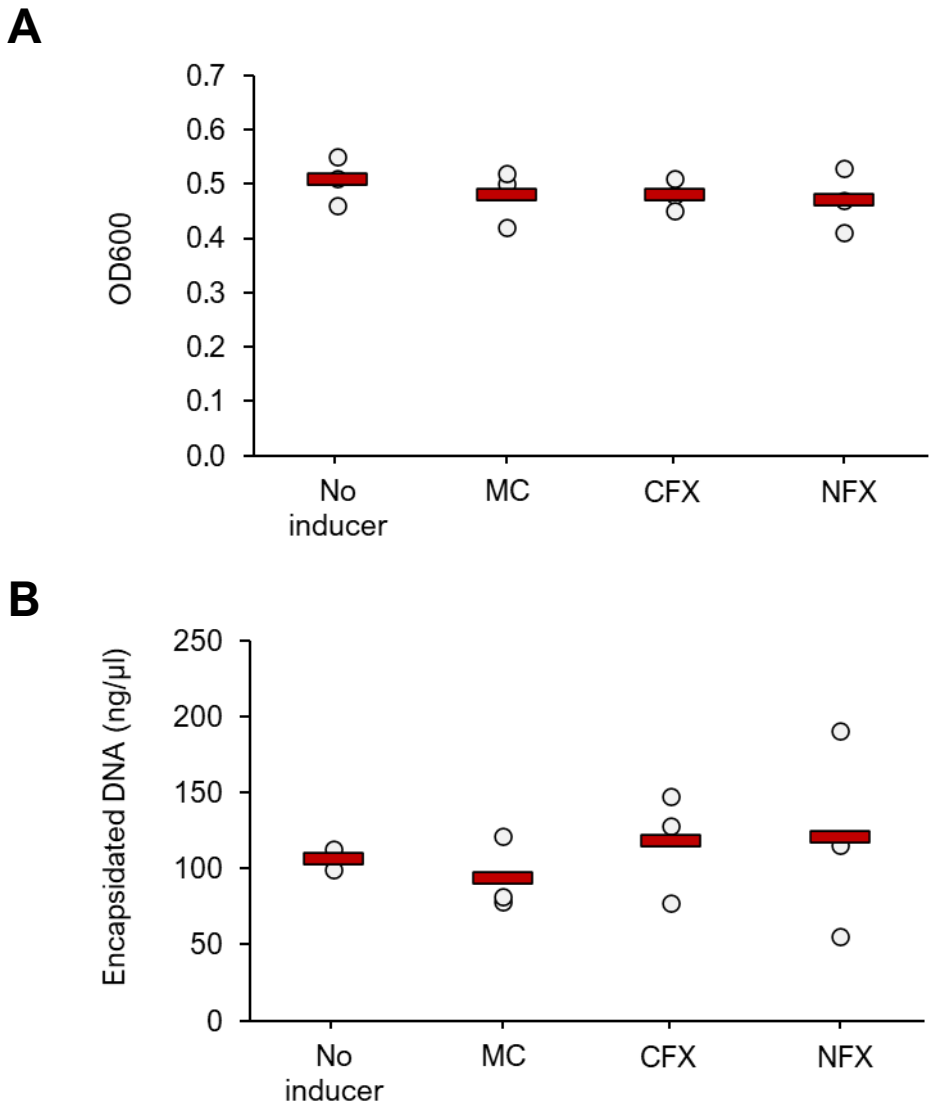

Figure 3: Common SOS-response inducing agents are not potent inducers of *C. clostridioforme* LM41 prophages. *C. clostridioforme* LM41 cultures were induced with common SOS-response-inducing chemicals, mitomycin C (MC), ciprofloxacin (CFX) or norfloxacin (NFX) and grown for 16-18 h at 37ºC in anaerobic conditions. An uninduced control sample was also included. OD600 values were obtained for each culture after 16-18 h to determine if phage-induced lysis had occurred (**A**) and encapsidated DNA was purified and quantified for each culture (**B**). Data points are from three independent experiments (n = 3), with mean values shown as red bars. All data were tested for significance using a one-way ANOVA with Tukey post-hoc tests; no statistically significant differences were observed between the groups (p>0.05).

bioRxiv preprint doi: https://doi.org/10.1101/2024.02.29.582698; this version posted February 29, 2024. The copyright holder for this preprint (which was not certified by peer review) is the author/funder, who has granted bioRxiv a license to display the preprint in perpetuity. It is made available under aCC-BY-NC-ND 4.0 International license.

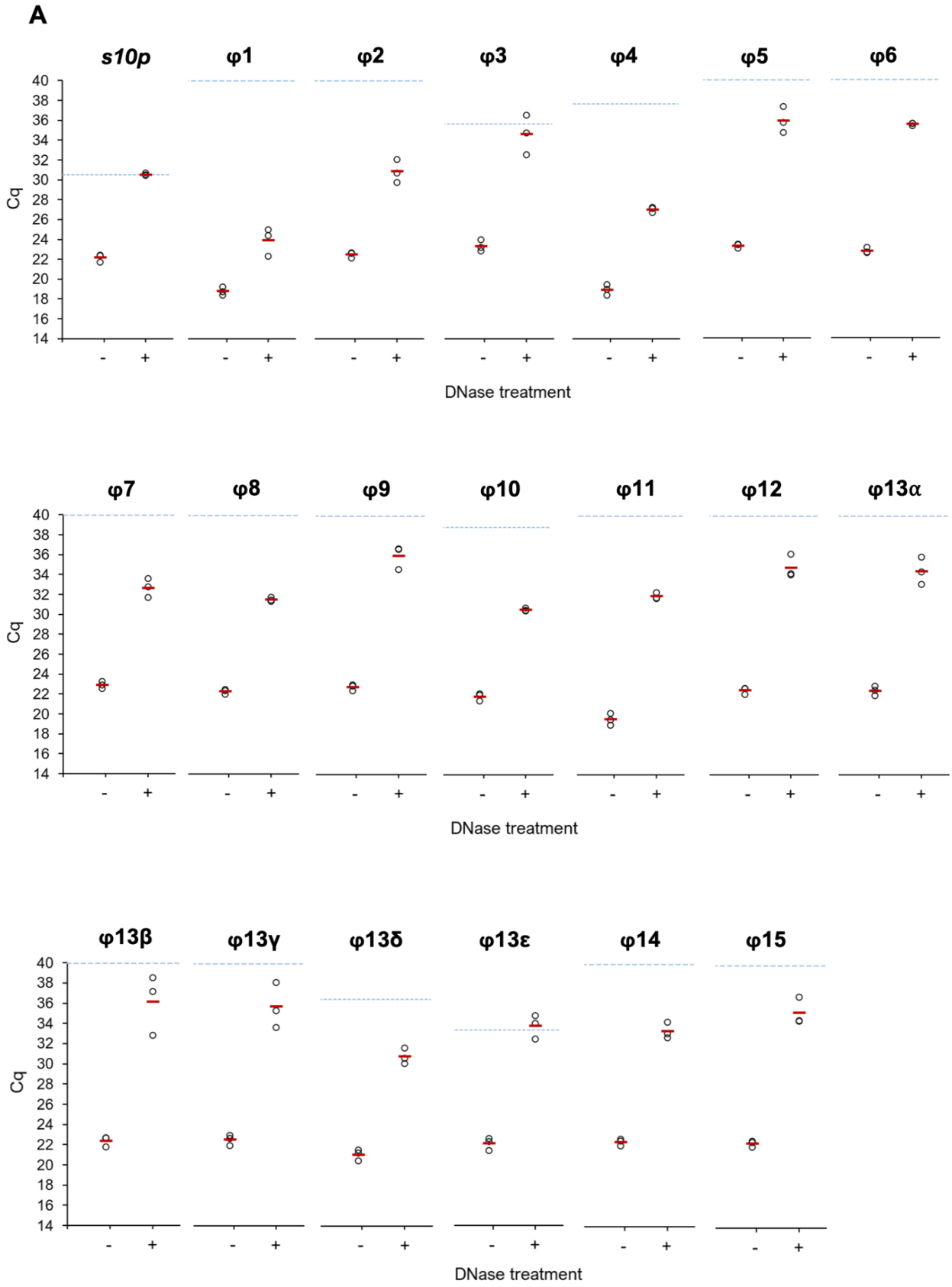

778

779

bioRxiv preprint doi: https://doi.org/10.1101/2024.02.29.582698; this version posted February 29, 2024. The copyright holder for this preprint (which was not certified by peer review) is the author/funder, who has granted bioRxiv a license to display the preprint in perpetuity. It is made available under aCC-BY-NC-ND 4.0 International license.

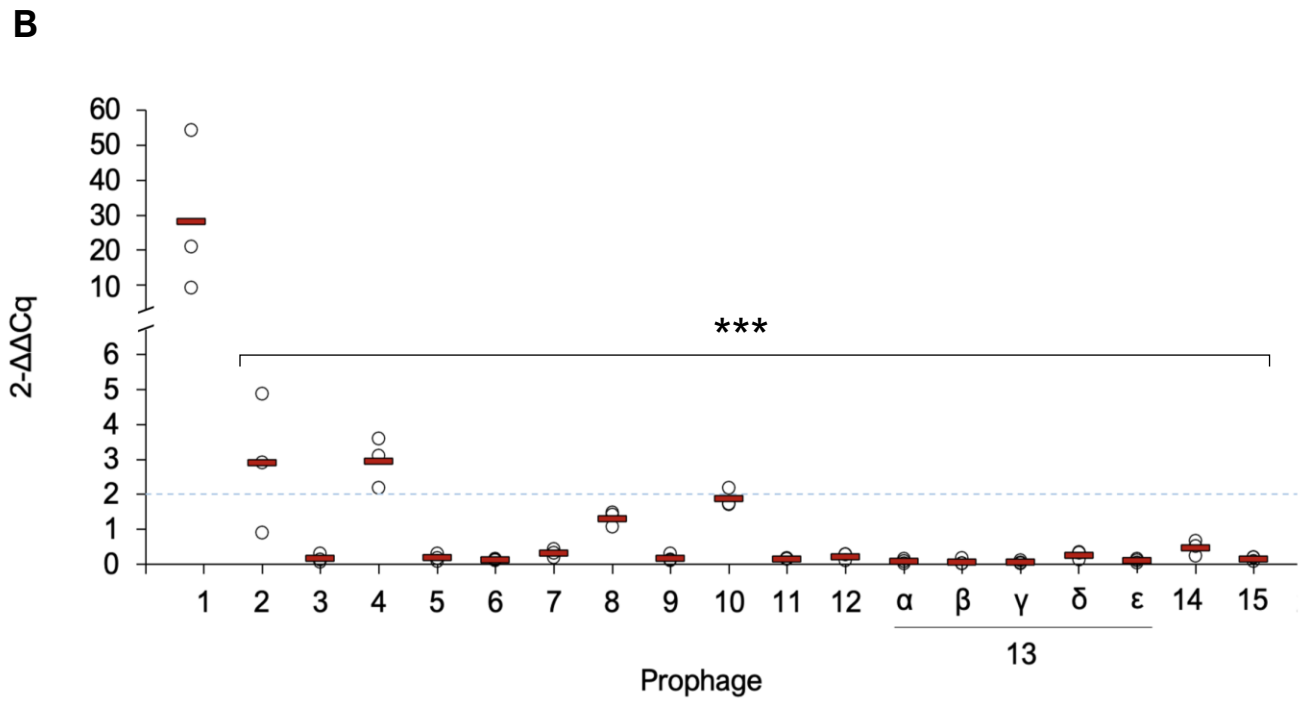

780

781 **Figure 4: Basal release of *C. clostridioforme* LM41 prophages under non-inducing**
782 **conditions.** *C. clostridioforme* LM41 was diluted 1:50 from an overnight culture into standard
783 FAB and grown for 24h under anaerobic conditions. Sterile filtered supernatants were subject
784 to either no treatment or digestion with 10 µg/ml DNase I for 1.5h. 1 µl of DNase-treated or
785 control supernatant was used as template for qPCR. *C. clostridioforme s10p* (equivalent to
786 *rpsJ*) was used as the housekeeper and as a marker for the presence of bacterial DNA. **A.**
787 Raw Cq values for the different target sequences. Data points are from 3 independent
788 experiments with mean values shown as red bars. No template control Cq values for each
789 target are shown by the dashed blue line. **B.** Fold-change in Cq of phage DNA in supernatant
790 samples following DNase treatment to remove non-encapsidated DNA. The ΔCq values for all
791 target samples were normalised using the ΔCq for the *s10p* gene (DNase treated Cq –
792 untreated Cq), and fold changes were calculated using the $2^{-\Delta\Delta Cq}$ calculation. Data points are
793 from 3 independent experiments with mean values shown as red bars. The dashed blue line
794 indicates 2-fold change threshold for reference. Asterisks denote statistically significant
795 differences between the mean $2^{-\Delta\Delta Cq}$ values for φ1 and the other phages, tested using a

bioRxiv preprint doi: https://doi.org/10.1101/2024.02.29.582698; this version posted February 29, 2024. The copyright holder for this preprint (which was not certified by peer review) is the author/funder, who has granted bioRxiv a license to display the preprint in perpetuity. It is made available under aCC-BY-NC-ND 4.0 International license.

repeated measures ANOVA with Tukey post-hoc tests (no Greisenham correction), where *p* values ranged <0.0001-0.0002.

bioRxiv preprint doi: https://doi.org/10.1101/2024.02.29.582698; this version posted February 29, 2024. The copyright holder for this preprint (which was not certified by peer review) is the author/funder, who has granted bioRxiv a license to display the preprint in perpetuity. It is made available under aCC-BY-NC-ND 4.0 International license.

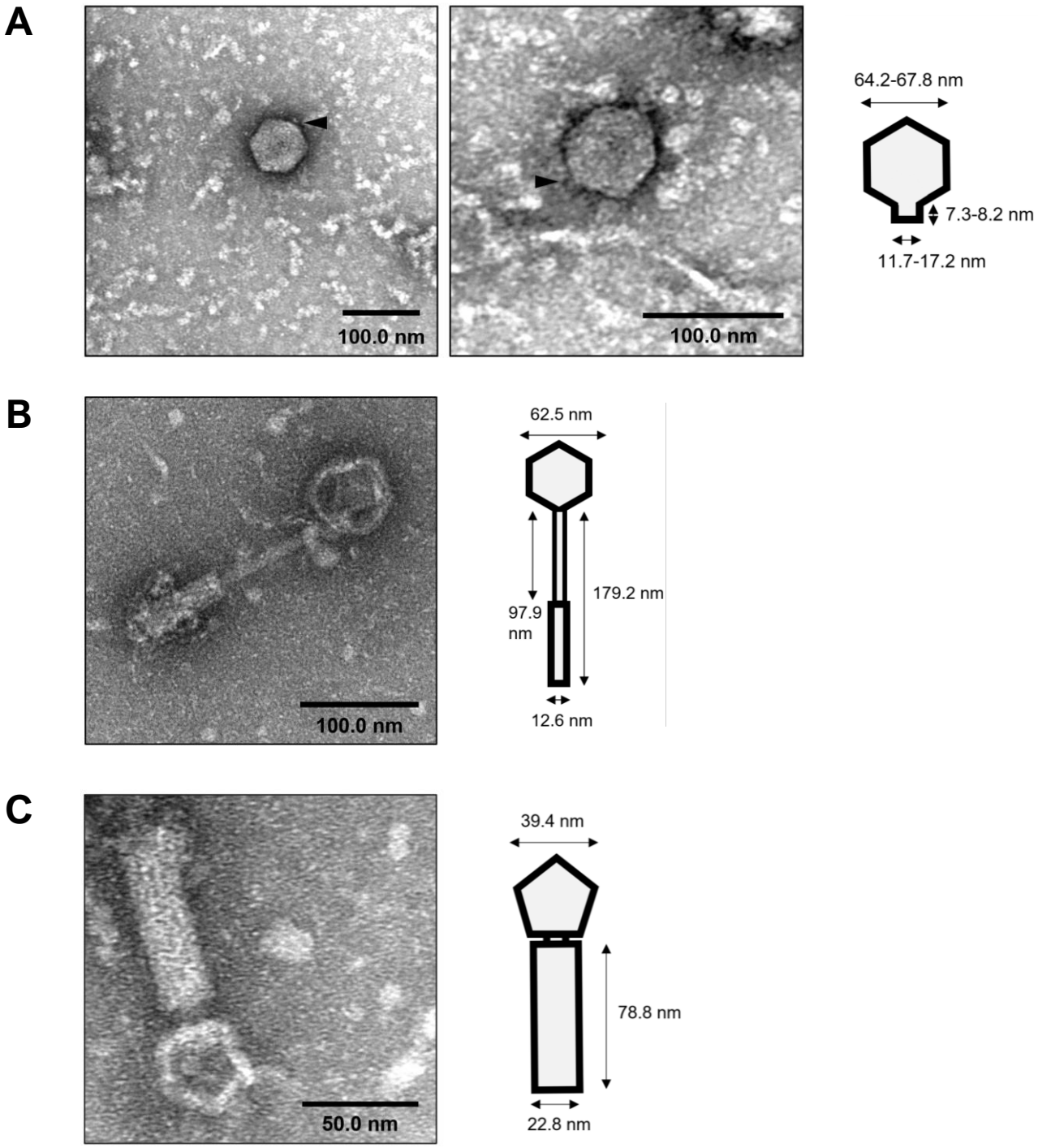

817

818 **Figure 5: TEM examination of LM41 culture supernatant reveals phage particles.**
819 *C. clostridioforme* LM41 was diluted 1:50 from an overnight culture into standard FAB and
820 grown for 24 h under anaerobic conditions. Sterile filtered supernatants were subject to
821 digestion with 10 µg/ml DNase I for 1.5 h to remove non-encapsidated DNA, then concentrated
822 following 10% PEG, 1 M NaCl precipitation. Samples were fixed and negatively stained with

bioRxiv preprint doi: https://doi.org/10.1101/2024.02.29.582698; this version posted February 29, 2024. The copyright holder for this preprint (which was not certified by peer review) is the author/funder, who has granted bioRxiv a license to display the preprint in perpetuity. It is made available under aCC-BY-NC-ND 4.0 International license.

0.5% (w/v) uranyl formate on copper-coated carbon grids, then imaged using a JEOL 1400 Flash TEM running at 80 kV. Particle dimensions for putative podoviruses (panel A) and tailed particles (panels B and C) are indicated on the schematics. Putative tail projections are indicated by black triangles (panel A).

bioRxiv preprint doi: https://doi.org/10.1101/2024.02.29.582698; this version posted February 29, 2024. The copyright holder for this preprint (which was not certified by peer review) is the author/funder, who has granted bioRxiv a license to display the preprint in perpetuity. It is made available under aCC-BY-NC-ND 4.0 International license.

827 **Table 1: Oligonucleotides used in this study**

Primer name	Sequence (5'-3')	Expected product (bp)
s10p-q-F	AGGATCACAGGTGAGCGGAC	146
s10p-q-R	GGCTTGGAGCTGTGATGTCG	
LM41phi1-q-F	ACAGCCAGAAAGCGAGCAGA	134
LM41phi1-q-R	TGTCCAGTGATTGCTCCGCA	
LM41phi2-q-F	TATTCTGGCCCTGCTGACGG	129
LM41phi2-q-R	TAGCCCATGACCGCCTCAAG	
LM41phi3-q-F	GGAAGCGGCGAACCTAAAGC	92
LM41phi3-q-R	TATACAGCCCGTGGAAGCCG	
LM41phi4-q-F	TCGGCCAACTCATTCAATGCT	142
LM41phi4-q-R	CGCAAGATGACGAGACAGCAC	
LM41phi5-q-F	AGTCGCTGGATACGCTGGAC	100
LM41phi5-q-R	TCCGTATCCGTCAAGGTCGC	
LM41phi6-q-F	GATACGGCCAGGGAGCTTGT	130
LM41phi6-q-R	CGGCGAAGGTGTATCCGTCT	
LM41phi7-q-F	GTATCAAAAGCGGCAGGGGC	106
LM41phi7-q-R	TACCGGGATACTCCGCTCCA	
LM41phi8-q-F	CCAGATAGCGGCAAAGCAGC	154
LM41phi8-q-R	GTATGCCTCCAGCGGTTCCT	
LM41phi9-q-F	GGAACGCCAACCCGTGGATA	140
LM41phi9-q-R	GCATGGTTCATCCGCCCAAG	
LM41phi10-q-F	AGCTGCTGCCGAGTTTCTGA	179
LM41phi10-q-R	GTAAGTGCATACGCGCCACC	
LM41phi11-q-F	ACGCCGGATAAAGGAAGGGG	131
LM41phi11-q-R	CCCCGTGATAGGCCATGGTT	
LM41phi12-q-F	GCGGCGGATTCAGAAACTGG	89
LM41phi12-q-R	CTATCGTGCCGTCCCGTCTT	
LM41phi13α-q-F	AGGTGTTTGCTTCCCACGGA	151
LM41phi13α-q-R	AATGCCCCTACTGATCCGCC	
LM41phi13β-q-F	CGCTGTATGGCAAAGGGCAG	161
LM41phi13β-q-R	AGACCCCGTTACCAGCATCG	
LM41phi13γ-q-F	ATTAACCCGGCGGATGTGGT	143
LM41phi13γ-q-R	ATAGGCTCCTGTCGCTGCTG	
LM41phi13δ-q-F	GCATGCTGCATTGTACCGCT	182
LM41phi13δ-q-R	CGTCCGCTGCTGTCAGGATA	
LM41phi13ε-q-F	CTGACGGCCAGGATAAGGCA	172
LM41phi13ε-q-R	GCCTGAATCAAGCGGCTGTC	
LM41phi14-q-F	AGCTCCAAGCCAAAGCGGTA	121
LM41phi14-q-R	CCCCGCTGTGTTCTTACGGA	

bioRxiv preprint doi: https://doi.org/10.1101/2024.02.29.582698; this version posted February 29, 2024. The copyright holder for this preprint (which was not certified by peer review) is the author/funder, who has granted bioRxiv a license to display the preprint in perpetuity. It is made available under aCC-BY-NC-ND 4.0 International license.

LM41phi15-q-F	CATGCGGCGGCAGATAACTT	155
LM41phi15-q-R	TTCCACTGCTCTCTCGCACG	

828

Table 2: *C. clostridioforme* LM41 prophage region characteristics

Phage	Location in LM41 genome	Genome size (bp)	DNA strand	Tail features				Closest relative (BLASTn)			
				Baseplate wedge subunit	Tail tape Measure	Sheath	Prediction	Description	Identity (%)	Cover (%)	Accession
φ1	194,517 - 235,362	40,846	Forward	Orf61	ND	ND	Podovirus	Caudoviricetes sp. isolate ctRvb1, partial genome	94.43	37	BK050138.1
φ2	301,574 - 342,165	40,592	Forward	ND	Orf65, Orf66	ND	Siphovirus	Caudoviricetes sp. isolate ctdym5, partial genome	95.39	40	BK055266.1
φ3	1,072,300 - 1,120,599	48,300	Forward	Orf64	Orf59	Orf55	Myovirus	Enterocloster bolteae strain CBBP-2	97.5	95	CP053229.1
φ4	1,281,572 - 1,323,457	41,690	Forward	Orf63	ND	ND	Podovirus	LM41φ1	99.02	74	N/A
φ5	3,073,910 - 3,122,116	48,207	Reverse	ND	Orf58	ND	Siphovirus	Blautia pseudococcoides strain SCSK	79.12	30	CP053228.1
φ6	3,448,526 – 3,490,199	41,674	Reverse	ND	Orf52	ND	Siphovirus	Caudoviricetes sp. isolate cthCz6, partial genome	93.24	38	BK022268.1
φ7	3,885,600 – 3,901,899	16,300	Reverse	ND	ND	ND	-	Caudoviricetes sp. isolate ct1dI13, partial genome	78.11	58	BK021065.1
φ8	3,846,360 - 3,885,591	39,232	Reverse	Orf47, Or48	ND	Orf39	Myovirus	Caudoviricetes sp. isolate ctELP1	79.38	65	BK049563.1
φ9	3,997,064 - 4,063,629	66,566	Reverse	ND	Orf133	ND	Siphovirus	Caudoviricetes sp. isolate ctRyL7, partial genome	91.04	68	BK049246.1
φ10	4,120,662 - 4,165,801	45,140	Reverse	Orf80, Orf81	Orf75	Orf71	Myovirus	Caudovirales sp. isolate ctjI31, partial genome	93.81	71	BK029493.1
φ11	5,193,058 – 5,226,919	33,862	Reverse	ND	Orf53	ND	Siphovirus	Caudoviricetes sp. isolate ctpXm10, partial genome	92.98	48	BK024821.1
φ12	6,190,004 - 6,237,536	47,533	Forward	ND	Orf63	ND	Siphovirus	Enterocloster bolteae strain ATCC BAA-613 chromosome	89.09	39	CP022464.2
φ13	6,632,999 - 6,769,447	136,449	Forward					N/A	N/A	N/A	N/A

α	6,632,999 - 6,684,039	51,041	Forward	ND	Orf65	ND	Siphovirus	Siphoviridae sp. isolate ctgM31, partial genome	92.9	75	BK028648.1
β	6,684,149 - 6,706,426	22,278	Forward	ND	ND	ND	-	Caudoviricetes sp. isolate ct1iX6, partial genome	81.66	26	BK023115.1
γ	6,706,413 - 6,714,990	8,578	Forward	ND	ND	ND	-	Lachnoclostridium sp. YL32 chromosome, complete genome	95.82	96	CP015399.2
δ	6,715,266 - 6,749,468	34,203	Forward	Orf174	Orf184, Orf185	Orf180	Myovirus	Lachnoclostridium sp. YL32 chromosome, complete genome	97.62	53	CP015399.2
ε	6,750,116 - 6,769,447	19,332	Forward	ND	Orf227	ND	Siphovirus	Siphoviridae sp. ctquf9, partial genome	86.92	88	BK014815.1
φ14	7,473,893 - 7,529,677	55,785	Forward	Orf65	Orf61	Orf57	Myovirus	No matches with coverage > 1%	N/A	N/A	N/A
φ15	7,532,147 - 7,579,680	47,534	Forward	Orf72	Orf68	Orf63	Myovirus	Lachnoclostridium sp. YL32 chromosome, complete genome	90.62	46	CP015399.2

ND, Not detected

bioRxiv preprint doi: https://doi.org/10.1101/2024.02.29.582698; this version posted February 29, 2024. The copyright holder for this preprint (which was not certified by peer review) is the author/funder, who has granted bioRxiv a license to display the preprint in perpetuity. It is made available under aCC-BY-NC-ND 4.0 International license.

Table 2: Prophage-encoded accessory Orfs of interest

Prophage	ORF	Annotation[1]	PHROG ID	Predicted product	Putative function
1	4	eggNOG-mapper	-	Dextransucrase activity	Host metabolism
	52	PHANOTATE	1048	Anti-CRISPR[2]	Anti-phage defence
	64	PHANOTATE	-	Hypothetical protein	Unknown
2	4	PHANOTATE	87	IrrE family metalloendopeptidase	Lysogeny regulation
	51	PHANOTATE	1423	Reverse transcriptase	Phage replication; Diversity generation
3	13	eggNOG-mapper	2889	PFAM Formylglycine-generating sulfatase enzyme	Host metabolism
	25	PHANOTATE	28876	Metal-dependent phosphohydrolase	Host metabolism
	71	eggNOG-mapper	2889	PFAM Formylglycine-generating sulfatase enzyme	Host metabolism
	73	PHANOTATE	3206	Avd protein of DGR	Diversity generation
	76	PHANOTATE	1423	Reverse transcriptase	Phage replication; Diversity generation
4	55	PHANOTATE	-	Anti-CRISPR[2]	Anti-phage defence
	67	PHANOTATE	-	Hypothetical protein	Unknown
5	1	Iterative search	-	Amidoligase enzyme	Host metabolism; Phage defence
	4	eggNOG-mapper	16694	Type I restriction-modification system R subunit	Phage defence
	5	eggNOG-mapper	-	Type I restriction modification DNA specificity domain	Phage defence
	8	eggNOG-mapper	-	Type I restriction modification DNA specificity domain	Phage defence
	9	eggNOG-mapper	-	Type I restriction modification DNA specificity domain	Phage defence
	10	eggNOG-mapper	2668	Type I restriction modification DNA specificity domain	Phage defence
	11	eggNOG-mapper	2713	Type I restriction-modification system methyltransferase subunit	Phage defence
	12	eggNOG-mapper	19315	IrrE N-terminal-like domain	Lysogeny regulation
	33,34	PHANOTATE	1384	Mom-like DNA modification protein	Anti-phage defence
	60	eggNOG-mapper	-	Chloramphenicol phosphotransferase-like protein	Resistance against ribosomal peptidyltransferases
	63	eggNOG-mapper	32044	Toxin SymE, type I toxin-antitoxin system	Translation repression
6	20	PHANOTATE	1423	Reverse transcriptase	Phage replication; Diversity generation
	30	PHANOTATE	424	Phosphoadenosine phosphosulfate reductase	Host metabolism
8	57	PHANOTATE	1423	Reverse transcriptase	Phage replication; Diversity generation
	60	PHANOTATE	937	Haemolysin	Host fitness/Cell lysis
9	27	PHANOTATE	392	Metal-dependent hydrolase	Host metabolism
	48	PHANOTATE	424	Phosphoadenosine phosphosulfate reductase	Host metabolism
	102	PHANOTATE	16724	Endonuclease; PHROG indicative of toxin element of TA system	Phage defence
	110	PHANOTATE	1384	Mom-like DNA modification protein	Anti-phage defence
	111	PHANOTATE	10089	DarB-like antirestriction	Anti-phage defence
	124	Iterative search	1048	Anti-CRISPR[2]	Anti-phage defence
	149	PHANOTATE	937	Haemolysin	Host fitness/Cell lysis

bioRxiv preprint doi: https://doi.org/10.1101/2024.02.29.582698; this version posted February 29, 2024. The copyright holder for this preprint (which was not certified by peer review) is the author/funder, who has granted bioRxiv a license to display the preprint in perpetuity. It is made available under aCC-BY-NC-ND 4.0 International license.

10	2	PHANOTATE	497	Toxin-antitoxin system HicB-like	Phage defence
	3	PHANOTATE	353	HicA toxin	Phage defence
	49	Iterative search	-	Lar-like restriction alleviation protein	Anti-phage defence
12	4	PHANOTATE	87	IrrE family metalloendopeptidase	Lysogeny regulation
	78	PHANOTATE	1423	Reverse transcriptase	Phage replication; Phage defence
13(α)	5	eggNOG-mapper	-	Acetyltransferase	Host metabolism
	28	eggNOG-mapper	32044	Toxin SymE, type I toxin-antitoxin system	Translation repression
	35,37	PHANOTATE	2443	Amidoligase enzyme	Host metabolism; Phage defence
	39	PHANOTATE	2520	Gamma-glutamyl cyclotransferase	Host metabolism
	50	eggNOG-mapper	2737	Addiction module antitoxin, RelB DinJ family	Phage defence
	51	eggNOG-mapper	2455	ParE toxin of type II toxin-antitoxin system, parDE	Phage defence
13(β)	83	PHANOTATE	310	Transposase	Phage replication
	84	PHANOTATE	296	DNA transposition protein	Phage replication
	95	eggNOG-mapper	8929	Transposase DDE domain	Phage replication
	96	eggNOG-mapper	34740	PFAM transposase, IS4 family protein	Phage replication
	98	eggNOG-mapper	12132	Reverse transcriptase (RNA-dependent DNA polymerase)	Phage replication; Diversity generation
	104	eggNOG-mapper	34860	Antitoxin component of a toxin-antitoxin (TA) module	Anti-phage defence
	105	eggNOG-mapper	-	RM system: HsdM N-terminal domain	Phage defence
	106	eggNOG-mapper	3830	RM system: DNA specificity	Phage defence
	107	eggNOG-mapper	1468	RM system: Type III restriction	Phage defence
13(**δ**)	140	PHANOTATE	310	Mu transposase, C-terminal	Phage replication
	141	PHANOTATE	296	DNA transposition protein	Phage replication
	149	PHANOTATE	424	Phosphoadenosine phosphosulfate reductase	Host metabolism;
	155	PHANOTATE	4681	Antitoxin from a toxin-antitoxin system	Anti-phage defence
13(ε)	206,208	PHANOTATE	2443	Amidoligase enzyme	Host metabolism; Phage defence
	210	PHANOTATE	2520	Gamma-glutamyl cyclotransferase	Host metabolism
14	40,42	PHANOTATE	424, 2302	Phosphoadenosine phosphosulfate reductase	Host metabolism
	73	PHANOTATE	1423	Reverse transcriptase	Phage replication; Diversity generation

[1]Annotation was performed using PHANOTATE (Pharokka) or eggNOG-mapper/iterative search with mmseqs against the PHROG database (PhageScope). PHANOTATE annotation calling was given priority for ORF function prediction over PhageScope unless no function could be assigned.
[2]Identified as encoding an anti-CRISPR protein by PhageScope using Anti-CRISPRdb.

bioRxiv preprint doi: https://doi.org/10.1101/2024.02.29.582698; this version posted February 29, 2024. The copyright holder for this preprint (which was not certified by peer review) is the author/funder, who has granted bioRxiv a license to display the preprint in perpetuity. It is made available under aCC-BY-NC-ND 4.0 International license.

Supplementary Figures

Supplementary Figure 1: Confirmation of DNase activity against *C. clostridioforme* LM41 genomic DNA. 200 ng of *C. clostridioforme* LM41 genomic DNA was treated with (T) or without (UT) 10 µg/ml DNase I for 30 min at 37ºC in parallel with culture supernatant sample digests (Figures 3 and 4) to confirm enzymatic activity. Samples were mixed with 10X loading dye and loaded on a 1% (w/v) TAE gel to run for 1.5 h at 120 V. 250 ng of 1 KB Plus DNA ladder (Invitrogen) was also loaded (M). The image shown is representative for each independent experiment performed.